THE JOURNAL OF BIOLOGICAL CHEMISTRY VOL. 289, NO. 30, pp. 20677–20693, July 25, 2014

A Combined "Omics" Approach Identifies N-Myc Interactor as a Novel Cytokine-induced Regulator of IRE1α Protein and c-Jun N-terminal Kinase in Pancreatic Beta Cells*

Received for publication, April 3, 2014, and in revised form, June 13, 2014 Published, JBC Papers in Press, June 16, 2014, DOI 10.1074/jbc.M114.568808

Flora Brozzi[‡], Sarah Gerlo[§¶1], Fabio Arturo Grieco[‡], Tarlliza Romanna Nardelli[‡‖], Sam Lievens[§¶], Conny Gysemans[2], Lorella Marselli[‡‡], Piero Marchetti[‡‡], Chantal Mathieu[**3], Jan Tavernier[§¶4], and Décio L. Eizirik[‡5]**

*From the [‡]Laboratory of Experimental Medicine and Center for Diabetes Research, Université Libre de Bruxelles, B-1070 Brussels, Belgium, the [§]Department of Medical Protein Research, Flanders Interuniversity Institute for Biotechnology (VIB), 9000 Gent, Belgium, the [¶]Department of Biochemistry, Ghent University, 9000 Gent, Belgium, the [‖]Laboratory of Endocrine Pancreas and Metabolism, University of Campinas, 13083-970 Campinas, São Paulo, Brazil, the **Laboratory of Clinical and Experimental Endocrinology, KULeuven, 3000 Leuven, Belgium, and the [‡‡]Department of Clinical and Experimental Medicine, Islet Cell Laboratory, University of Pisa, 56126 Pisa, Italy*

Background: Cytokine-induced IRE1α activation regulates adaptive/pro-apoptotic endoplasmic reticulum (ER) stress transition in type 1 diabetes (T1D).
Results: The IRE1α-binding protein NMI modulates JNK activation and apoptosis in beta cells.
Conclusion: NMI induction is a novel negative feedback mechanism regulating ER stress and apoptosis in cytokine-exposed beta cells.
Significance: Clarifying cytokine modulation of ER stress may provide information to protect beta cells in early T1D.

Type 1 diabetes is an autoimmune disease with a strong inflammatory component. The cytokines interleukin-1β and interferon-γ contribute to beta cell apoptosis in type 1 diabetes. These cytokines induce endoplasmic reticulum stress and the unfolded protein response (UPR), contributing to the loss of beta cells. IRE1α, one of the UPR mediators, triggers insulin degradation and inflammation in beta cells and is critical for the transition from "physiological" to "pathological" UPR. The mechanisms regulating inositol-requiring protein 1α (IRE1α) activation and its signaling for beta cell "adaptation," "stress response," or "apoptosis" remain to be clarified. To address these questions, we combined mammalian protein-protein interaction trap-based IRE1α interactome and functional genomic analysis of human and rodent beta cells exposed to pro-inflammatory cytokines to identify novel cytokine-induced regulators of IRE1α. Based on this approach, we identified N-Myc interactor (NMI) as an IRE1α-interacting/modulator protein in rodent and human pancreatic beta cells. An increased expression of NMI was detected in islets from nonobese diabetic mice with insulitis and in rodent or human beta cells exposed *in vitro* to the pro-inflammatory cytokines interleukin-1β and interferon-γ. Detailed mechanistic studies demonstrated that NMI negatively modulates IRE1α-dependent activation of JNK and apoptosis in rodent and human pancreatic beta cells. In conclusion, by using a combined omics approach, we identified NMI induction as a novel negative feedback mechanism that decreases IRE1α-dependent activation of JNK and apoptosis in cytokine-exposed beta cells.

Type 1 diabetes (T1D)[6] is a chronic autoimmune disease characterized by pancreatic islet inflammation (insulitis) and progressive beta cell loss (1, 2). During this inflammatory process, there is an ongoing "dialogue" between invading immune cells and the target beta cells. This dialogue is mediated by both cytokines/chemokines produced by immune cells and beta cells and by immunogenic signals delivered by dying or modified beta cells (1), and it is modulated by the genetic background of the affected individuals (3).

Pro-inflammatory cytokines produced by the islet-infiltrating immune cells, such as IL-1β, TNF-α, and IFN-γ, induce endoplasmic reticulum (ER) stress in both rodent and human islet cells, triggering the unfolded protein response (UPR) (4, 5). Markers of the UPR are present in islets from T1D patients (6) and in immune-mediated nonobese diabetic (NOD) mice (7, 8).

* This work was supported in part by Juvenile Diabetes Research Foundation International Grant 17-2013-515, European Union Projects NAMIT and BetaBat, in the Framework Programme 7 of the European Community, Actions de Recherche Concertée de la Communauté Française, and the Fonds National de la Recherche Scientifique, Belgium.
[1] Postdoctoral fellow of the Research Foundation-Flanders and supported by the Ghent University GROUP-ID Multidisciplinary Research Platform.
[2] Supported by the Katholieke Universiteit Leuven and the seventh Framework Program of the European Union with Natural Immunomodulators as Novel Immunotherapies for Type 1 Diabetes.
[3] Clinical researcher from the Flemish Research Foundation (Fonds Voor Wetenschappelijk Onderzoek Vlaanderen).
[4] Recipient of a European Research Council advanced grant.
[5] To whom correspondence should be addressed: Laboratory of Experimental Medicine and ULB Center for Diabetes Research, Université Libre de Bruxelles, Route de Lennik, 808-CP618, B-1070 Brussels, Belgium. Tel.: 322-555-6242; Fax: 32-2-555-6239; E-mail: deizirik@ulb.ac.be.

[6] The abbreviations used are: T1D, type 1 diabetes; ER, endoplasmic reticulum; UPR, unfolded protein response; MAPPIT, mammalian protein-protein interaction trap; NMI, N-Myc interactor; NOD, nonobese diabetic; CPA, cyclopiazonic acid; ANOVA, analysis of variance; Epo, erythropoietin; IP, immunoprecipitation.

Recent findings indicate that a mild ER stress amplifies IL-1β-induced nuclear factor κB (NF-κB) signaling, with consequent increase in local inflammation (9) and beta cell apoptosis (10). Importantly, *in vivo* modulation of ER stress by use of chemical chaperones prevents autoimmune diabetes in two mouse models of the disease (8).

In rat beta cells, cytokine-dependent activation of the UPR occurs via NO-dependent inhibition of the sarcoendoplasmic reticulum pump Ca^{2+}-ATPase 2b (SERCA-2b), ER calcium decrease, and unfolded protein accumulation (4). These events, however, seem to differ among species (11), and other unknown mechanisms are implicated in cytokine-induced UPR activation in human pancreatic beta cells.

The three main sensors of the UPR are the transmembrane proteins inositol-requiring protein 1α (IRE1α), protein kinase RNA-like endoplasmic reticulum kinase (PERK), and activating transcription factor 6 (ATF6) (12). These proteins detect the accumulation of unfolded proteins in the ER lumen and activate mechanisms to restore ER function (12–14). In case of chronic and/or severe ER stress, persistent activation of the UPR triggers apoptosis (15, 16), contributing to the loss of beta cells in type 1 (6, 7, 8, 17) and type 2 diabetes (18). What determines the transition from "physiological" to "pathological" UPR remains to be clarified (13), but accumulating evidence indicates that the amplitude and duration of IRE1α signaling is critical for this transition (19).

Once IRE1α is activated, its cytoplasmic domain is autophosphorylated and gains endoribonuclease activity, cleaving 26 nucleotides from the mRNA encoding X-box binding protein 1 (*Xbp1*). This generates a spliced variant (Xbp1s) that functions as a potent transcription factor, regulating genes involved in protein folding, maturation, quality control, and protein degradation via the ER-associated degradation pathway (12, 18). IRE1α degrades ER-targeted mRNAs, such as insulin mRNA in pancreatic beta cells (20, 21), thus decreasing the production of new proteins (20–22). IRE1α also activates c-Jun N-terminal kinase (JNK) through the binding of the adaptor protein TNF receptor-associated factor 2 (TRAF2) (23). IRE1α activation is regulated and fine-tuned by both signals derived from the ER lumen (12) and by the formation of protein complexes between its cytosolic domain and regulatory proteins (13, 19, 24). Several cytosolic IRE1α-regulating proteins have been described (24, 25), but little is known regarding IRE1α regulation in pancreatic beta cells (13, 25, 26).

Against this background, the aim of this study was to identify novel cytokine-induced IRE1α-interacting proteins that modulate UPR activation in pancreatic beta cells. For this goal, we used a high throughput mammalian two-hybrid technology, MAPPIT (mammalian protein-protein interaction trap) that is based on complementation of a modified cytokine receptor complex. This allows screening of a bait of interest against an arrayed prey collection derived from the CCSB Human ORFeome collection (27). The MAPPIT-based IRE1α interactome analysis identified N-Myc interactor (NMI) as an IRE1α interacting/modulator protein. This novel role for NMI was confirmed in rodent and human pancreatic beta cells, and an increased expression of NMI was detected in islets from NOD mice with insulitis and in rodent and human beta cells exposed *in vitro* to pro-inflammatory cytokines. Of particular relevance, cytokine-induced NMI modulates IRE1α-dependent activation of JNK and apoptosis in pancreatic beta cells.

TABLE 1
Characteristics of the human islet donors

Subject	Age	Gender	Body mass index	Beta cell purity
	years		*kg/m²*	*%*
C1	84	F	26	73
C2	59	M	25	70
C3	68	M	37	57
C4	59	M	27	58
C5	68	M	28	42
C6	76	F	25	30
C7	79	M	25	85
C8	85	M	25	39
C9	69	M	25.1	68
C10	82	M	23	61
C11	69	F	20.8	70
C12	40	M	32.9	37
C13	64	F	29.4	47
C14	58	F	21.3	67
C15	81	M	27.8	63
C16	64	F	29.3	67
C17	47	F	29.4	58
$X \pm$ S.E.	67.8 ± 3.1		26.9 ± 1	58 ± 3.6%

EXPERIMENTAL PROCEDURES

Culture of Human Islet Cells, FACS-purified Rat Beta Cells, INS-1E Cells, the Human Beta Cell Line EndoC-βH1, and HEK293T Cells—Human islets from 17 nondiabetic donors were isolated in Pisa using collagenase digestion and density gradient purification (28). The donors (7 women and 10 men) were 67.8 ± 3.1 years old and had a body mass index of 26 ± 1.2 (kg/m²) (Table 1). Beta cell purity, as evaluated by immunofluorescence for insulin, using a specific anti-insulin antibody (Table 2), was 58 ± 3.6%. The islets were cultured in M199 culture medium containing 5.5 mM glucose and sent to Brussels, Belgium, within 1–5 days after isolation, where they were dispersed and cultured in Ham's F-10 medium containing 6.1 mM glucose (Invitrogen) as described (29, 30).

Isolated pancreatic islets of male Wistar rats (Charles River Laboratories, Brussels, Belgium) were dispersed, and beta cells were purified by autofluorescence-activated cell sorting (FACSAria, BD Biosciences) (31). Beta cells (93 ± 2% purity as evaluated by immunofluorescence for insulin; $n = 12$) and dispersed rat islet cells were cultured in Ham's F-10 medium containing 10 mM glucose, 2 mM glutamine, 50 μM 3-isobutyl-L-methylxanthine, 0.5% fatty acid-free bovine serum albumin (BSA) (Roche Applied Science), 5% heat-inactivated fetal bovine serum (FBS, Qualified, Invitrogen), 50 units/ml penicillin, and 50 μg/ml streptomycin (31). The same medium but without FBS was used during cytokine exposure. The rat insulin-producing INS-1E cell line, kindly provided by Dr. C. Wollheim, University of Geneva, Switzerland, was cultured in RPMI 1640 GlutaMAX-I medium (Invitrogen) (32).

The human beta cell line EndoC-βH1, kindly provided by Dr. R. Scharfmann, University of Paris, France (33), was cultured in DMEM containing 5.6 mM glucose, 2% BSA fraction V, 50 μM 2-mercaptoethanol (Sigma), 10 mM nicotinamide (Calbiochem), 5.5 μg/ml transferrin, 6.7 ng/ml selenite (Sigma), 100 units/ml penicillin, and 100 μg/ml streptomycin (Lonza, Leus-

TABLE 2
Antibodies used in the study

Antibody	Company	Reference	Dilution
Insulin	Sigma	I2018	1:1000
Donkey anti-mouse IgG rhodamine	Lucron Bioproducts, De Pinte, Belgium	715-026-156	1:200
IRE1α	Santa Cruz Biotechnology, Santa Cruz CA	Sc-20790	IP, 1 mg/ml
IRE1α	Cell Signaling, Danvers, MA	3294	1:1000 for WB
FLAG® M2	Sigma	F1804	1:1000
NMI	Santa Cruz Biotechnology	Sc-22819	1:100 for IHC
NMI	Aviva Systems Biology Corp., San Diego	ARP35736	1:1000 for WB
HRP-conjugated anti-rabbit IgG	Lucron Bioproducts	711-036-152	1:5000 for WB
HRP-conjugated anti-mouse IgG	Lucron Bioproducts	715-036-150	1:5000 for WB
Alexa Fluor 488 goat anti-mouse	Invitrogen	A-11008	1:500
Alexa Fluor 546 goat anti-rabbit	Invitrogen	A-11030	1:500
TRAF2	Cell Signaling	4712	1:1000 for WB
MKK7	Cell Signaling	4172	1:1000 for WB
β-Actin	Cell Signaling	4967	1:5000
α-Tubulin	Sigma	T9026	1:5000

den, The Netherlands). The same medium, but with 2% FBS, was used during the cytokine treatment as described (34). The human embryonic kidney cells HEK293T were cultured in DMEM containing 25 mM glucose, 5% FBS, 100 units/ml penicillin, 100 μg/ml streptomycin, and sodium pyruvate 100× (Invitrogen).

Cell Treatment and Nitric Oxide (NO) Measurement—INS-1E cells were exposed to 12.5 μM cyclopiazonic acid (CPA) (Sigma), a concentration previously shown by us to induce ER stress in these cells (10). CPA was dissolved in dimethyl sulfoxide (DMSO), which was used as control condition at the concentration of 0.03%. The following cytokine concentrations were used, based on previous dose-response experiments performed by our group (29, 35–37) as follows: recombinant human IL-1β (R&D Systems, Abingdon, UK) 10 units/ml for INS-1E cells or 50 units/ml for human islet cells, primary rat beta cells, dispersed rat islet cells, and the human beta cell line EndoC-βH; recombinant rat IFN-γ (R&D Systems) 100 units/ml for INS-1E cells or 500 units/ml for dispersed rat islet cells and primary rat beta cells; human IFN-γ (PeproTech, London, UK) 1000 units/ml for human islet cells or the human beta cell line EndoC-βH; recombinant murine TNF-α (Innogenetics, Gent, Belgium) 1000 units/ml for all cell types. Lower cytokine concentration and shorter time points were used in the rodent experiments because rat beta cells are more sensitive to cytokine-induced damage than human islets (38, 39). Culture medium was collected for nitrite determination (nitrite is a stable product of NO oxidation) by the Griess method (40).

Array MAPPIT and Binary MAPPIT—To identify IRE1α-interacting proteins, an array MAPPIT screen was performed as described (27), using as MAPPIT bait the cytoplasmic portion of IRE1α (amino acids 571–977). Briefly, HEK293T cells expressing the IRE1α bait protein were reverse-transfected in 384-well plate format with a collection of ~10,000 full ORFs from the Version 5.1 ORFeome collection that were Gateway-cloned as MAPPIT preys. Two independent screens were performed, and after elimination of nonspecific binders (*i.e.* binders that appear as "positive" also in irrelevant screens), 31 putative IRE1α-interacting proteins were selected.

In the binary MAPPIT analyses, an IRE1α bait containing the cytoplasmic portion of IRE1α was generated based on the original pSEL MAPPIT bait construct (41). This bait contains the extracellular part of the human erythropoietin receptor and the transmembrane and intracellular parts of the mouse leptin receptor. MAPPIT preys were cloned in the previously described pMG1 vector (42). Briefly, HEK293T cells were transfected with bait, prey, and STAT3 reporter plasmids (Table 3) by the use of a standard calcium phosphate transfection method, and luciferase activity was measured 48 h after transfection using the Luciferase assay system kit (Promega, Leiden, The Netherlands) on a TopCount luminometer. Cells were stimulated with erythropoietin (5 ng/ml) 24 h after transfection. Luciferase data were represented as average relative light units ± S.E. of three technical transfection replicates. To confirm equal expression of empty and IRE1α-cyto baits, the MAPPIT signal with the REM2 prey protein (which interacts with the leptin receptor portion of the bait) was measured. Additional selection of IRE1α-interacting proteins for subsequent study in pancreatic beta cells was done by systematic comparison against previous RNA-seq and array analysis of cytokine-treated human and rodent beta cells, as described under "Results" and Fig. 1.

TABLE 3
Plasmids used in the study

Plasmids	Encoding protein
NMI-FLAG	NMI FLAG-tagged at the C-terminal domain
IRE1α-V5	IRE1α V5-tagged at the C-terminal domain
pSEL-IRE1α bait	Cytosolic domain of IRE1α
pSEL-IRE1K599A bait	Cytosolic domain of IRE1α with K599A mutation
pSEL-empty bait	Empty
pMG1-NMI prey	NMI
pMG1-empty prey	Empty
pXP2d2-rPAP1	Luciferase STAT3 reporter plasmid
pMG1-REM2	RAS (RAD and GEM)-like GTP-binding 2 protein (REM2)

RNA Interference and Transfection with Plasmids—The siRNAs used in the study are described in Table 4. The optimal concentration of siRNA used for cell transfection (30 nM) was established previously (29, 43). Cells were transfected using the Lipofectamine RNAiMAX lipid reagent (Invitrogen) as described previously (43, 44). All Stars Negative Control siRNA (Qiagen, Venlo, The Netherlands) was used as negative control (siCTRL). This siCTRL does not affect beta cell gene expression or insulin release, as compared with nontransfected cells (43). After 16 h of transfection, cells were cultured for a 24- or 48-h recovery period before exposure to cytokines.

The plasmids used in the study are described in Table 3. HEK293T were transfected with 1 μg of plasmid using Lipo-

TABLE 4
siRNAs used in the study

Name	Type	Distributors	Sequence
siCTRL	Allstar Negative Control siRNA	Qiagen, Venlo, The Netherlands	Not provided
Rat siNMI	BLOCK-iT Stealth™ Select siRNA	Invitrogen	1, 5′-GAGAAUGUACCAGAAAGAAAGCUUA-3′ 2, 5′-UAAGCUUUCUUUCUGGUACAUUCUC-3′
Rat siNMI (second siRNA)	BLOCK-iT Stealth™ Select siRNA	Invitrogen	1, 5′-CCAUUUAUAGAAAGACGCUUGGAAA-3′ 2, 5′-UUUCCAAGCGUCUUUCUAUAAAUGG-3′
Human siNMI #1	BLOCK-iT Stealth™ Select siRNA	Invitrogen	Not provided
Human siNMI #2	BLOCK-iT Stealth™ Select siRNA	Invitrogen	Not provided
Rat siIRE1α	ON-TARGETplus	Thermo Scientific, Chicago	1, CUGAUGACUUCGUGCGCUA 2, GGCCAGCAGAUUAGCGAAU 3, CAGACAAGCACGAGGACGU 4, AAGAUGGACUGGCGGGAGA
Rat siTRAF2	BLOCK-iT Stealth™ Select siRNA	Invitrogen	Not provided
Rat siMKK7	FlexiTubes iRNA Rn_Map2k7_3	Qiagen	5′-CGGACGUCUUUAUUGCCAUTT-3′

TABLE 5
Sequence of the primers used in the study

Primer	Forward sequence	Reverse sequence
NMI (human)	5′-CAGCGACAGTTTCGAGAACC-3′	5′-ATCACGAGGTCAGGAGATCG-3′
β-Actin (human)	5′-CTGTACGCCAACACAGTGCT-3′	5′-GCTCAGGAGGAGCAATGATC-3′
Nmi (rat)	5′-GGATGGAGACCATTTCTCAAATAG-3′	5′-CTTCTTCCTTCTCAAAGGTGATAAG-3′
Ins-2 (rat)	5′-TGTGGTTCTCACTTGGTGGA-3′	5′-CTCCAGTTGTGCCACTTGTG-3′
Dp5 (rat)	5′-GCCGTGGTGTTACTTGGA-3′	5′-GATTGTGCCAGAGCTTCACA-3′
Gapdh (rat)	5′-AGTTCAACGGCACAGTCAAG-3′	5′-TACTCAGCACCAGCATCACC-3′
Xbp1 spliced (rat)	5′-GAGTCCGCAGCAGGTG-3′	5′-GTGTCAGAGTCCATGGGA-3′
Maf-A (rat)	5′-AAGGAGGAGGTCATCCGACT-3′	5′-TCTGGAGCTGGCACTTCTCG-3′
Pdx1 (rat)	5′-GGTATAGCCAGCGAGATGCT-3′	5′-TCAGTTGGGAGCCTGATTCT-3′

fectamine 2000 lipid reagent (Invitrogen) according to the manufacturer's instructions.

Assessment of Cell Viability—The percentage of viable, apoptotic, and necrotic cells was determined after 15 min of incubation with the DNA-binding dyes propidium iodide (5 μg/ml; Sigma) and Hoechst dye 33342 (5 μg/ml; Sigma). A minimum of 600 cells was counted for each experimental condition by two independent observers, with one of them unaware of sample identity. The agreement between findings obtained by the two observers was always >90%. This fluorescence assay for single cells is quantitative and has been validated by systematic comparisons against electron microscopy observations, ladder formation, and caspase 3/9 activation (10, 29, 45, 46).

mRNA Extraction and Real Time PCR—Poly(A)$^+$ mRNA was isolated from cultured cells using the Dynabeads mRNA DIRECT™ kit (Invitrogen) and reverse-transcribed as described previously (31, 47). The real time PCR amplification reactions were done using iQ SYBR Green Supermix on a LightCycler instrument (Roche Applied Science) and on a Rotor-Gene Q (Qiagen), and the concentration of the gene of interest was calculated as copies per μl using the standard curve method (31, 48). Gene expression values in human and rat cells were corrected by respectively the housekeeping genes β-actin and *Gapdh,* whose expression is not modified in these cells by cytokine treatment (29, 49). The primers used in this study are provided in the Table 5.

Western Blot—After cell culture and treatment, cells were washed with cold PBS and lysed using Laemmli Sample Buffer. Total protein was extracted and resolved by 8–10% SDS-PAGE, transferred to a nitrocellulose membrane, and immunoblotted with the specific antibodies for the protein of interest (Table 2) as described (29). The intensity values for the proteins were corrected by the values of the housekeeping proteins α-tubulin or β-actin.

Immunoprecipitation—Proteins from transfected HEK293T cells were collected with cold lysis buffer (50 mM Tris, pH 7.5, 20 mM NaCl, 1% Nonidet P-40, 10 mM NaF, 1 mM Na_3VO_4, and Complete Protease inhibitor mixture, Roche Applied Science) and then precleared 1 h at 4 °C with protein G-Sepharose 4 Fast Flow (GE Healthcare). The same amount of protein was then incubated overnight at 4 °C, either with the anti-FLAG antibody or with the anti-IRE1α antibody (Santa Cruz Biotechnology, sc-20790). Normal mouse IgG (Santa Cruz Biotechnology, sc-2025) or normal rabbit IgG (sc-2027) were used as negative controls. After incubation for 1 h with Protein G-Sepharose 4 Fast Flow (GE Healthcare), the complexes were precipitated by centrifugation. The immunoprecipitates were washed five times with cold lysis buffer and then resuspended in 5× Laemmli Sample Buffer. Immunoprecipitates, total proteins, and flow-through were run in 8% SDS-PAGE, transferred to a nitrocellulose membrane, and immunoblotted with the specific antibodies for the protein of interest (Table 2).

Insulin Secretion—For determination of insulin secretion, INS-1E cells were incubated for 1 h in glucose-free RPMI GlutaMAX-I medium and then incubated for 30 min in Krebs-Ringer solution without glucose. Cells were then exposed to 1.7, 16.7, or 16.7 mM glucose + forskolin (20 μM) for 30 min. Dispersed rat islet cells were incubated for 30 min in Krebs-Ringer solution containing 1.7 mM glucose. Cells were then exposed to 1.7, 16.7, or 16.7 mM glucose + forskolin (20 μM) for 1 h. Total insulin was extracted with acidic ethanol. Insulin was measured by the rat insulin ELISA kit (Mercodia, Uppsala, Sweden).

Histology—Pancreata from BALB/c control mice and diabetes-prone NOD mice were collected at different ages, namely 4, 9, 13, and 17 weeks for BALB/c and 3, 8, 12, and 17 weeks for NOD mice, fixed in 4% formaldehyde, and then paraffin-embedded. 5-μm-thick sections were subjected to antigen

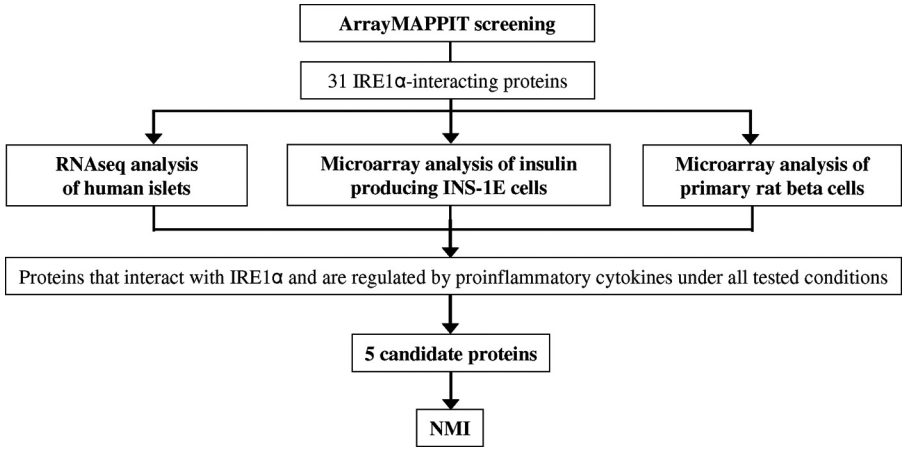

FIGURE 1. **Selection of IRE1α-interacting proteins.** The array MAPPIT screening identified 31 potential IRE1α-interacting proteins. These proteins were compared against our microarray and RNA sequencing data from cytokine-treated insulin-producing INS-1E cells (50), FACS-purified rat beta cells (51), and human islet cells (30). As a result of this analysis, five candidate proteins that interact with IRE1α and are regulated by pro-inflammatory cytokines under all tested conditions were selected. Additional selection, based on literature survey, indicated NMI as the best candidate for further studies.

retrieval by boiling the sections in 10 mM citrate buffer, pH 6, for 10 min. After overnight incubation at 4 °C with primary antibody against NMI, slides were double-stained with an anti-insulin antibody for 1 h at room temperature. Alexa Fluor fluorescent secondary antibodies (Invitrogen) were applied for 1 h at room temperature (Table 2). After nuclear staining with Hoechst, pancreatic sections were mounted with Fluorescence Mounting Medium (DAKO, Glostrup, Denmark). Immunofluorescence was visualized on a Zeiss microscope (Axio ImagerA1, Zeiss-Vision, Munich, Germany) equipped with a camera (AxioCAM Zeiss), as described previously (6). Images were acquired at room temperature using Zeiss/EC Plan Neofluar objective lenses at ×40 magnification and Axio Vision Zeiss software.

Ethic Statements—Human islet collection and handling were approved by the local Ethical Committee in Pisa, Italy.

Male Wistar rats were housed and used according to the guidelines of the Belgian Regulations for Animal Care. All experiments were approved by the local Ethical Committee.

NOD mice, originally obtained from Professor Wu (Department of Endocrinology, Peking Union Medical College Hospital, Beijing, China) were housed and inbred in the KULeuven animal facility since 1989. BALB/c mice were purchased from Harlan (Horst, The Netherlands). All experimental procedures in mice were approved and performed in accordance with the Ethics Committee of the KULeuven, Leuven, Belgium.

Statistical Analysis—Data are expressed as mean ± S.E. A significant difference between experimental conditions was assessed by one-way ANOVA followed by a paired Student's *t* test with Bonferroni correction. p values < 0.05 were considered statistically significant.

RESULTS

NMI Interacts with IRE1α—We have presently used ArrayMAPPIT to identify proteins that bind to the cytoplasmic domain of IRE1α. This generated a list of 31 putative IRE1α-interacting proteins.[7] These results were compared against our microarray and RNA sequencing data from insulin-producing INS-1E cells (50), FACS-purified rat beta cells (51), and human islet cells (30) exposed to stress signals that are relevant for type 1 diabetes, namely the pro-inflammatory cytokines IL-1β + IFN-γ (1, 29, 30).

Five candidate proteins that interact with IRE1α and are modified by pro-inflammatory cytokine treatment in pancreatic beta cells were identified. NMI was chosen as the most promising one following additional selection based on literature review (Fig. 1).

To confirm the interaction between NMI and IRE1α, a binary MAPPIT analysis was done (Fig. 2*a*). For this purpose HEK293T cells were co-transfected with an erythropoietin (Epo) receptor-based MAPPIT bait protein containing the cytoplasmic portion of IRE1α (pSEL-IRE1α), a FLAG-tagged NMI prey (pMG1-NMI), and a STAT3-responsive luciferase reporter (pXP2d2-rPAP1). After stimulation with Epo, there was a 100-fold increased luciferase signal as compared with cells co-transfected with the empty prey vector. In addition, although the empty MAPPIT bait produced an aspecific signal when combined with the NMI prey, the specific signal with the IRE1α bait was nearly 10-fold stronger (Fig. 2*a*). As a control for bait expression levels, the interaction of empty and IRE1α baits with the REM2 (RAD and GEM-like GTP Binding 2) prey, which is known to bind the intracellular cytokine receptor portion of the MAPPIT bait, was investigated and indicated equal bait expression. These data show that when IRE1α and NMI are present in the cells, they interact and reconstitute a functional STAT3-based reporter assay leading to the expression of luciferase.

Binary MAPPIT analysis was used to assess the ability of NMI to bind to the kinase-defective K599A IRE1α mutant (Fig. 2*b*) (52). For this purpose, MAPPIT bait containing the kinase-defective K599A IRE1α mutant (pSEL-IRE1α K599A) was added to the assay described above. After stimulation with Epo, a 50-fold increased luciferase signal was observed in both IRE1α WT and K599A IRE1α mutant when combined with the NMI prey, as compared with the control (empty prey vector) (Fig. 2*b*). This result shows similar ability of NMI to interact with

[7] S. Gerlo and J. Tavernier, unpublished data.

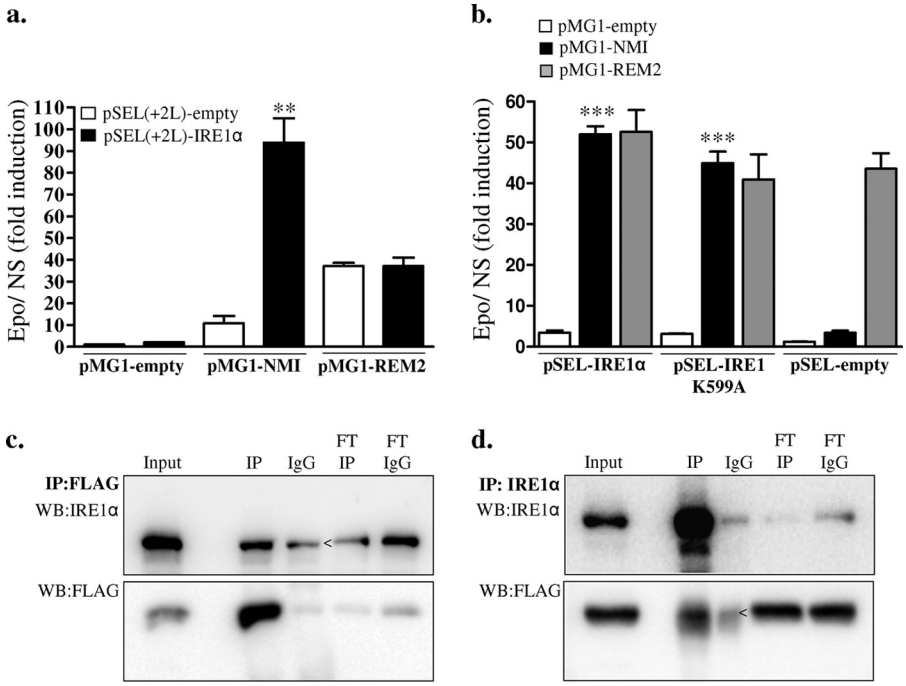

FIGURE 2. **IRE1α interacts with NMI.** The IRE1α-NMI interaction was confirmed by binary MAPPIT (*a* and *b*) and co-immunoprecipitation in HEK293T cells (*c* and *d*). For the binary MAPPIT analysis, HEK293T cells were transiently transfected with plasmids encoding pSEL(+2L)-IRE1α bait (*black bars*) or pSEL(+2L)-empty (*white bars*) together with an empty or a FLAG-tagged pMG1-NMI prey construct or a pMG1-REM2 prey construct (as indicated), combined with the pXP2d2-rPAP1-luciferase reporter (*a*). For binary MAPPIT with the kinase-defective K599A IRE1α mutant, HEK293T cells were transiently transfected with plasmids encoding pSEL(+2L)-IRE1α bait, pSEL(+2L)-IRE1αK599A bait, or pSEL(+2L)-empty bait (as indicated), together with an empty (*white bars*) or FLAG-tagged pMG1-NMI prey construct (*black bars*) and pMG1-REM2 prey construct (*gray bars*), combined with the pXP2d2-rPAP1-luciferase reporter (*b*). After 24 h, cells were left untreated or stimulated with Epo for 24 h. Luciferase counts of triplicate measurements are expressed as fold induction *versus* nonstimulated (*a* and *b*). HEK293T cells were co-transfected with plasmids encoding IRE1α-V5 and NMI-FLAG. After 48 h of transfection, proteins were collected for IP with anti-FLAG (*c*) or anti-IRE1α antibodies (*d*). Nonspecific IgG was used as a negative control. IPs and flow-through (*FT*) were analyzed by Western blot (*WB*) using anti-IRE1α and anti-FLAG antibodies, as indicated. < indicates nonspecific binding. **, $p < 0.01$ IRE1α baits *versus* empty baits; paired Student's *t* test (*a*). ***, $p < 0.001$ pMG1-NMI *versus* empty baits; one-way ANOVA (*b*). Data shown are mean ± S.E. of three independent experiments (*a* and *b*). The figures shown are representative of five (*c*) and two (*d*) independent experiments.

both IRE1α WT and the K599A mutant, suggesting that NMI-IRE1α interaction is independent on the phosphorylated state of IRE1α.

The interaction between NMI and IRE1α was further validated by co-immunoprecipitation experiments. HEK293T cells were co-transfected with IRE1α-V5 and NMI-FLAG-encoding plasmids and proteins collected and processed for immunoprecipitation. When proteins were immunoprecipitated with anti-FLAG antibody (Fig. 2*c*), IRE1α was detected in the immunoprecipitate (IP) as shown by Western blot analysis (Fig. 2*c*). In a mirror image of this experiment, immunoprecipitation of the proteins with an anti-IRE1α antibody (Fig. 2*d*) showed that the NMI-FLAG protein was present in the IP, whereas use of a nonspecific rabbit IgG (negative control) failed to detect NMI-FLAG protein (Fig. 2*d, 3rd lane* from *left*). The lack of NMI-FLAG signal or IRE1α signal from the flow-through of the NMI-FLAG IP or IRE1α IP, respectively, confirmed the reliability of the analysis.

Inflammation Increases NMI Expression in Pancreatic Islet Cells—We confirmed by real time-PCR (RT-PCR) our previous microarray findings (50, 51) indicating that pro-inflammatory cytokines induce NMI expression in rat insulin-producing cells. There was a peak of NMI expression after 24 h in INS-1E cells (Fig. 3*a*) and at 6 h in FACS-purified rat beta cells (Fig. 3*b*).

Importantly, these findings were reproduced in human islets by real time PCR (Fig. 3*c*) and Western blot (Fig. 3*d*) after a 48-h incubation with IL-1β + IFN-γ, confirming our previous RNA sequencing data (30). The increased expression of NMI in the clonal human beta cell line EndoC-βH1 after treatment with a different combination of pro-inflammatory cytokines (Fig. 3*e*) indicates that cytokine-induced NMI expression takes place at least in part at the pancreatic beta cell level.

To test whether increased NMI expression occurs during beta cell inflammation *in vivo*, we evaluated NMI expression in NOD mice, a well known animal model of autoimmune diabetes (7, 53). Immunofluorescence staining of pancreatic sections from NOD mice (Fig. 4*a*) showed NMI expression in insulin-positive cells at 8, 12, and 17 weeks (Fig. 4*a, panels E, H,* and *K,* and *F, I,* and *L*), whereas NMI was not detected in age-matched BALB/c mice islets (Fig. 4*b, panels E, H,* and *K*). Notably, NMI was not detected in NOD mouse islets at 3 weeks of age (Fig. 4*a, panels B* and *C*), when the islets are still free from the immune cell infiltration (7), and in the islets of NOD mice at 8 weeks of age that were insulitis-free (Fig. 4*c, panels B* and *C*), whereas islets from the same mice but with insulitis had clear up-regulation of NMI expression (Fig. 4*a, panels E* and *F*). Our data suggest that insulitis is associated with increased NMI expression in mouse beta cells *in vivo*.

NMI Inhibition Does Not Affect IRE1α Endonuclease Activity and Insulin Secretion in Pancreatic Beta Cells—To assess the function of cytokine-induced NMI expression on IRE1α activ-

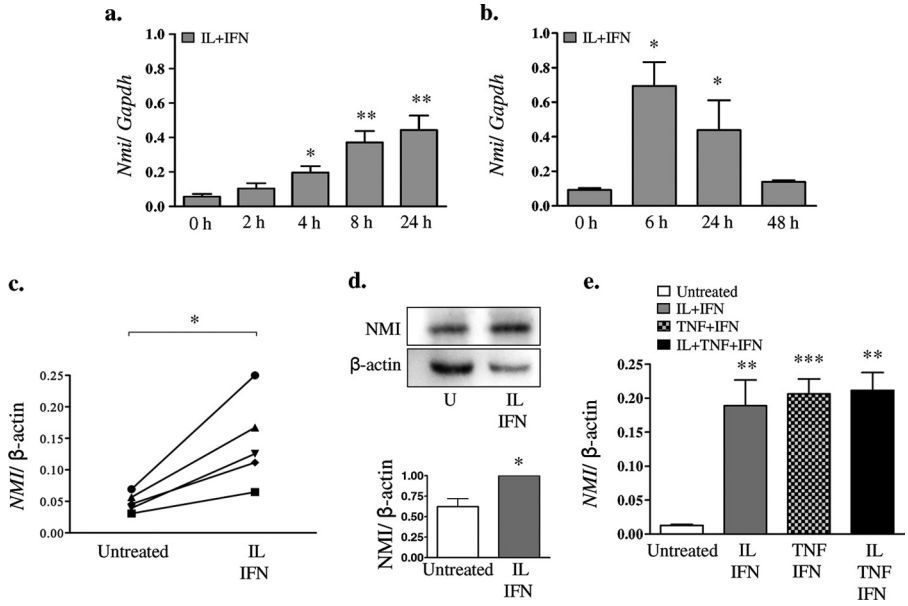

FIGURE 3. **IL-1β+IFN-γ induce NMI expression in rodent and human beta cells.** The expression of NMI was assessed by RT-PCR (*a–c* and *e*) and by Western blot (*d*) in INS-1E cells (*a*), FACS-purified rat beta cells (*b*), human islet cells (*c* and *d*), and the human beta cell line EndoC-βH1 cells (*e*) and normalized for the housekeeping gene *Gapdh* (*a* and *b*) or β-actin (*c–e*). Cells were left untreated (*white bar*) or treated with IL-1β + IFN-γ (IL + IFN, *gray bars*), TNF-α + IFN-γ (TNF + IFN, *checkerboard bar*), or IL-1β + TNF-α + IFN-γ (IL + TNF + IFN, *black bar*), as indicated. One representative Western blot for NMI in human islet cells and the mean ± S.E. of the optical density analysis of three independent experiments are shown (*d*). The cytokine exposure time was as indicated in *a* and *b* and at 48 h in *c, d* and *e*. *, $p < 0.05$; **, $p < 0.01$; ***, $p < 0.001$ *versus* 0 h or untreated (*U*); paired Student's *t* test. Data shown are mean ± S.E. of 3–5 independent experiments.

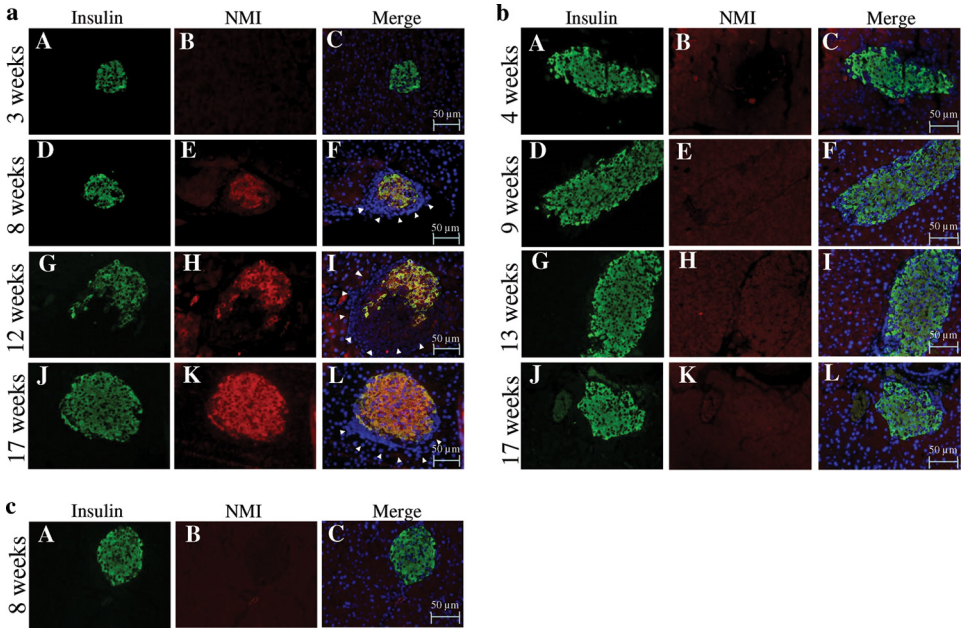

FIGURE 4. **Increased expression of NMI in inflamed islets from diabetes-prone NOD mice.** Pancreatic sections from 3-, 8-, 12-, and 17-week-old NOD mice were stained with antibodies specific for insulin (*panels A, D, G,* and *J, green*), NMI (*panels B, E, H,* and *K, red*), and with Hoechst for nuclear staining (*panels C, F, I,* and *L, blue*). The immunofluorescence analysis shows NMI expression in insulin-positive cells in NOD mice at 8, 12, and 17 weeks (*panels F, I,* and *L, yellow*), but not at 3 weeks (*panels B* and *C*). Infiltrated lymphocytes, a sign of insulitis, are indicated by *white arrowheads* (*panels F, I,* and *L*). Insulitis is present at 8, 12, and 17 weeks of age but not at 3 weeks. The images shown are representative of 14 ± 3 islet sections from three different mice per age (*a*). Pancreatic sections from 4-, 9-, 13-, and 17-week-old BALB/c mice were stained with antibodies specific for insulin (*panels A, D, G,* and *J, green*), NMI (*panels B, E, H,* and *K, red*), and with Hoechst for nuclear staining (*panels C, F, I,* and *L, blue*). Immunofluorescence analysis indicates the absence of NMI expression in insulin-positive cells in BALB/c mice (*panels C, F, I,* and *L, merge*). The images shown are representative of 21 ± 1 islet sections from three mice per age (*b*). Pancreatic sections from 8-week-old NOD mice were stained with antibodies specific for insulin (*panel A, green*), NMI (*panel B, red*), and with Hoechst (*panel C, blue*) for nuclear staining. Immunofluorescence analysis indicates the absence of NMI expression (*panel B*) in insulin-positive cells in NOD mouse islets without insulitis (*panel C, merge*) as compared with abundant NMI expression (*a, panel E*) in the presence of insulitis (*a, panel F, yellow*). The images shown are representative of 11–12 islet sections from three mice (*c*). *Bars,* 50 μm.

ity, we knocked down (KD) NMI with a specific siRNA (siNMI). NMI KD in INS-1E cells (Fig. 5, *a* and *b*) did not modify cytokine-induced IRE1α endonuclease activity as evaluated by *Xbp1* splicing (*Xbp1s*) (Fig. 5*c*) and *Ins-2* mRNA degradation (Fig. 5, *d* and *e*). These data were confirmed in FACS-purified rat beta cells, where NMI KD (>60% inhibition; Fig. 5*f*) did not change cytokine-induced IRE1α-dependent *Ins-2* mRNA degradation (Fig. 5*g*).

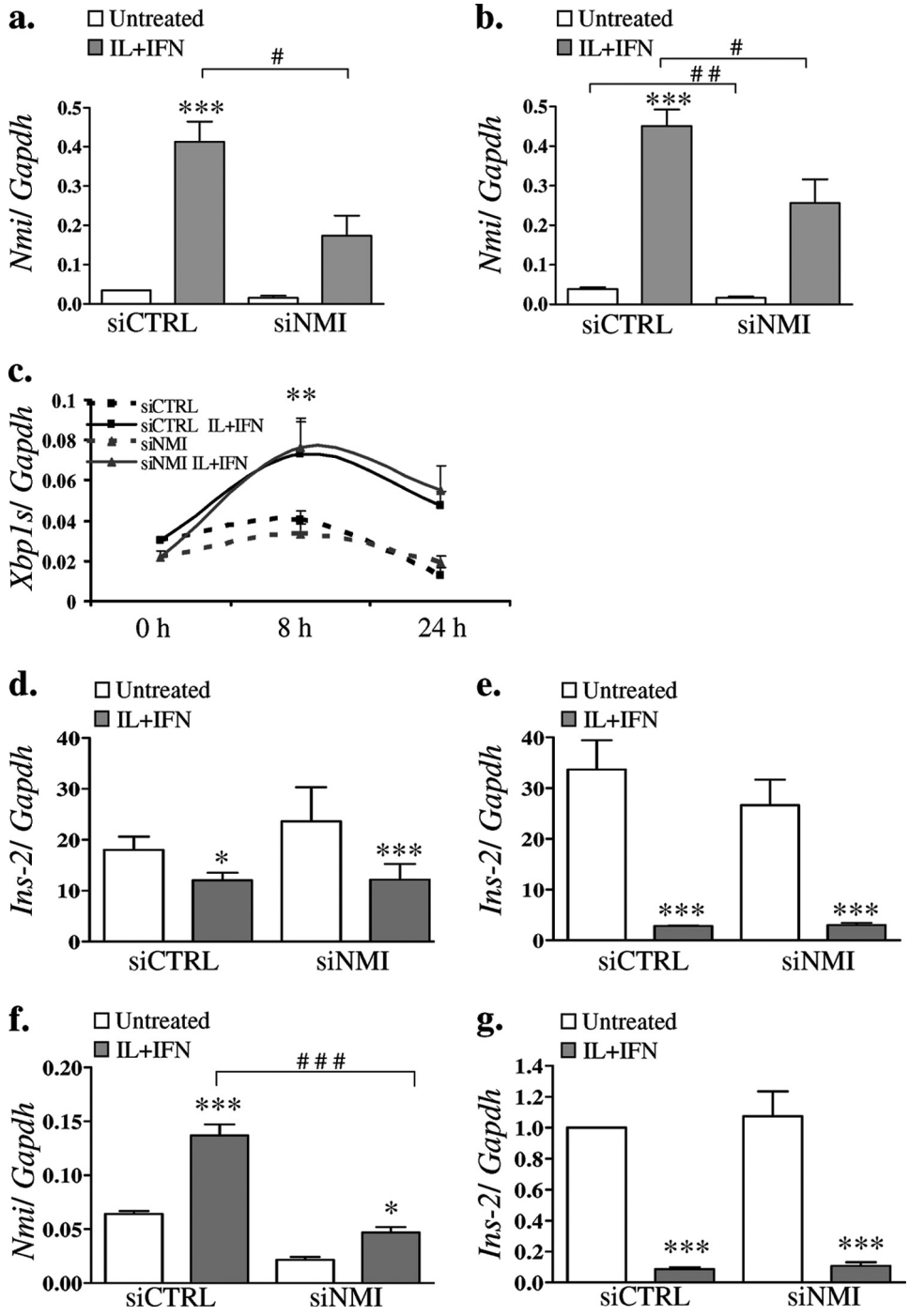

FIGURE 5. **NMI KD does not affect IRE1 endonuclease activity in IL-1β + IFN-γ-treated rodent beta cells.** INS-1E cells were transfected with siCTRL or siNMI. After 48 h, cells were left untreated (*white bars*) or treated with IL-1β + IFN-γ (IL + IFN, *gray bars*) for 8 (*a*) or 24 h (*b*). The expression of *Nmi* (*a* and *b*) was assessed by RT-PCR and normalized for the housekeeping gene *Gapdh*. The expression of *Xbp1* splicing (*Xbp1s*) was assessed by RT-PCR after 0, 8 and 24 h of IL-1β + IFN-γ treatment (*c*). INS-1E cells (*d* and *e*) and FACS-purified rat beta cells (*f* and *g*) were transfected with siCTRL or siNMI. After 48 h, cells were left untreated (*white bars*) or treated with IL-1β + IFN-γ (IL + IFN, *gray bars*) for 8 (*d*), 24 (*e*), or 48 h (*f* and *g*). The expression of *Nmi* (*f*) and *Ins-2* (*d, e,* and *g*) was assessed by RT-PCR, normalized for the housekeeping gene *Gapdh*. *, $p < 0.05$; **, $p < 0.01$, and ***, $p < 0.001$ IL + IFN *versus* respective untreated; #, $p < 0.05$; ##, $p < 0.01$ and ###, $p < 0.001$ as indicated by the *bars*; one-way ANOVA followed by Student's paired *t* test with Bonferroni correction. Data shown are mean ± S.E. of 3–5 independent experiments.

Glucose- and forskolin-stimulated insulin secretion did not change in INS-1E (Fig. 6*a*) and dispersed rat islet cells (Fig. 6*g*) after NMI KD (Fig. 6, *c* and *i*) both in untreated and cytokine-treated cells (Fig. 6, *a* and *g*). As expected, IL-1β + IFN-γ treatment inhibited insulin secretion in both INS-1E and dispersed rat islet cells (Fig. 6, *a* and *g*) and decreased total insulin content in both models (Fig. 6, *b* and *h*). INS-1E cells had a mild decrease in insulin content and expression in NMI KD compared with siCTRL in the untreated condition (Fig. 6, *b* and *d*), but this was not confirmed in primary rat islet cells, where *Ins-2*, *Maf-A* expression (Fig. 6, *j* and *k*), and total insulin protein content (Fig. 6*h*) were similar after

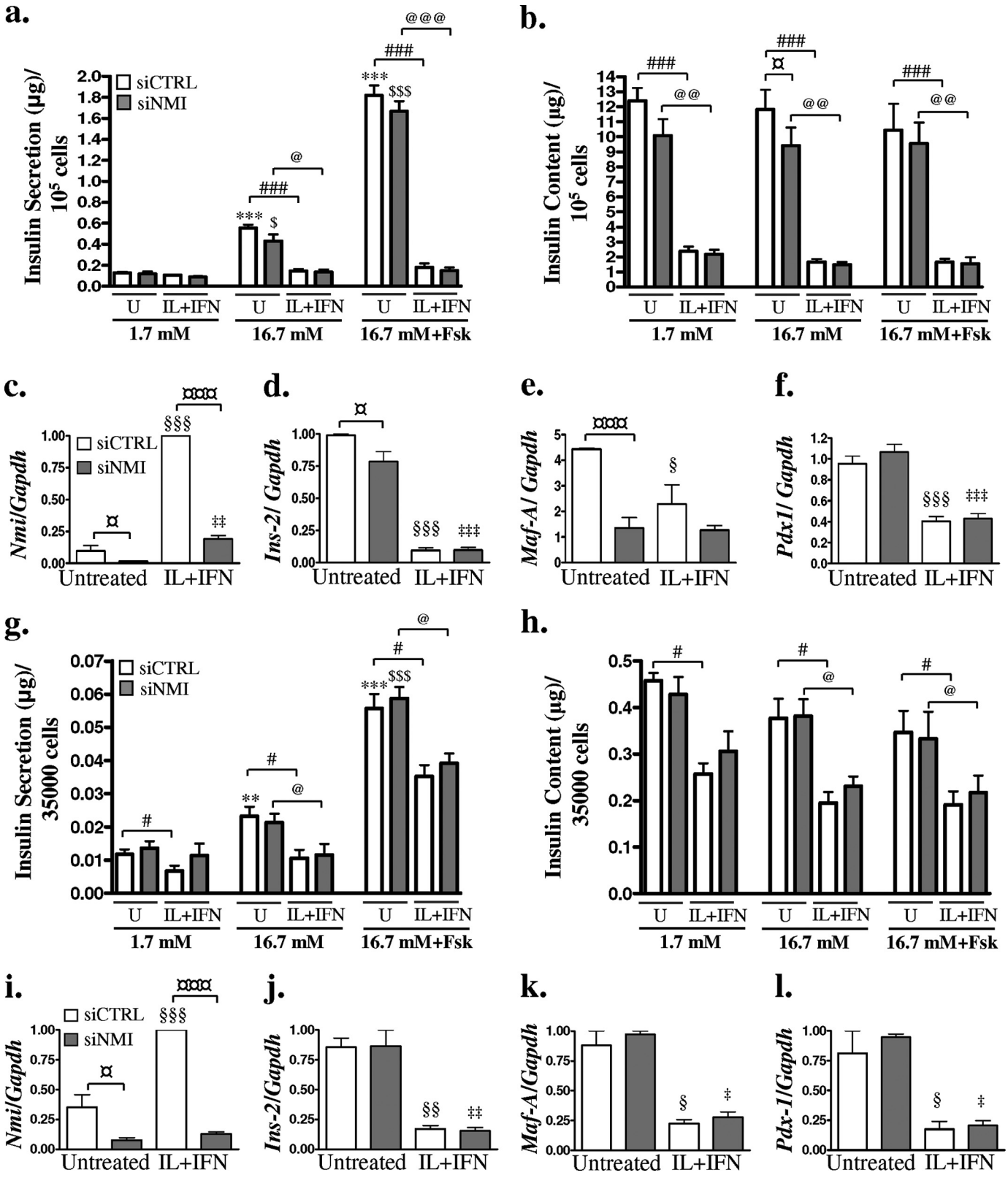

FIGURE 6. **NMI KD does not affect glucose- and forskolin-stimulated insulin secretion in INS-1E and dispersed rat islet cells.** INS-1E (*a–f*) and dispersed rat islet cells (*g–l*) were transfected with siCTRL (*white bars*) or siNMI (*gray bars*). After 48 h, cells were left untreated (*U*) or treated with IL-1β + IFN-γ (IL + IFN) for 24 h and used for insulin secretion studies. Insulin secretion and total insulin content of INS-1E (*a* and *b*) and dispersed rat islet cells (*g* and *h*) were measured after exposure to 1.7 mM glucose, 16.7 mM glucose, or 16.7 mM glucose + forskolin (20 µM) as indicated. The expression of *Nmi* (*c* and *i*), *Ins-2* (*d* and *j*), *Maf-A* (*e* and *k*), and *Pdx-1* (*f* and *l*) was assessed by RT-PCR and normalized for the housekeeping gene *Gapdh*. **, $p < 0.01$, and ***, $p < 0.001$, *versus* untreated siCTRL at 1.7 mM glucose; $, $p < 0.05$, and $$$, $p < 0.001$, *versus* untreated siNMI at 1.7 mM glucose; §, $p < 0.05$, §§, $p < 0.01$, and §§§, $p < 0.001$ *versus* siCTRL untreated; ‡, $p < 0.05$, ‡‡, $p < 0.01$, and ‡‡‡, $p < 0.001$, *versus* siNMI untreated; #, $p < 0.05$, ##, $p < 0.01$, and ###, $p < 0.001$; @, $p < 0.05$, @@, $p < 0.01$, and @@@, $p < 0.001$; ¤, $p < 0.05$; ¤¤, $p < 0.01$, and ¤¤¤, $p < 0.001$ as indicated by *bars*. One-way ANOVA followed by Student's paired *t* test with Bonferroni correction. Data shown are mean ± S.E. of 3–5 independent experiments.

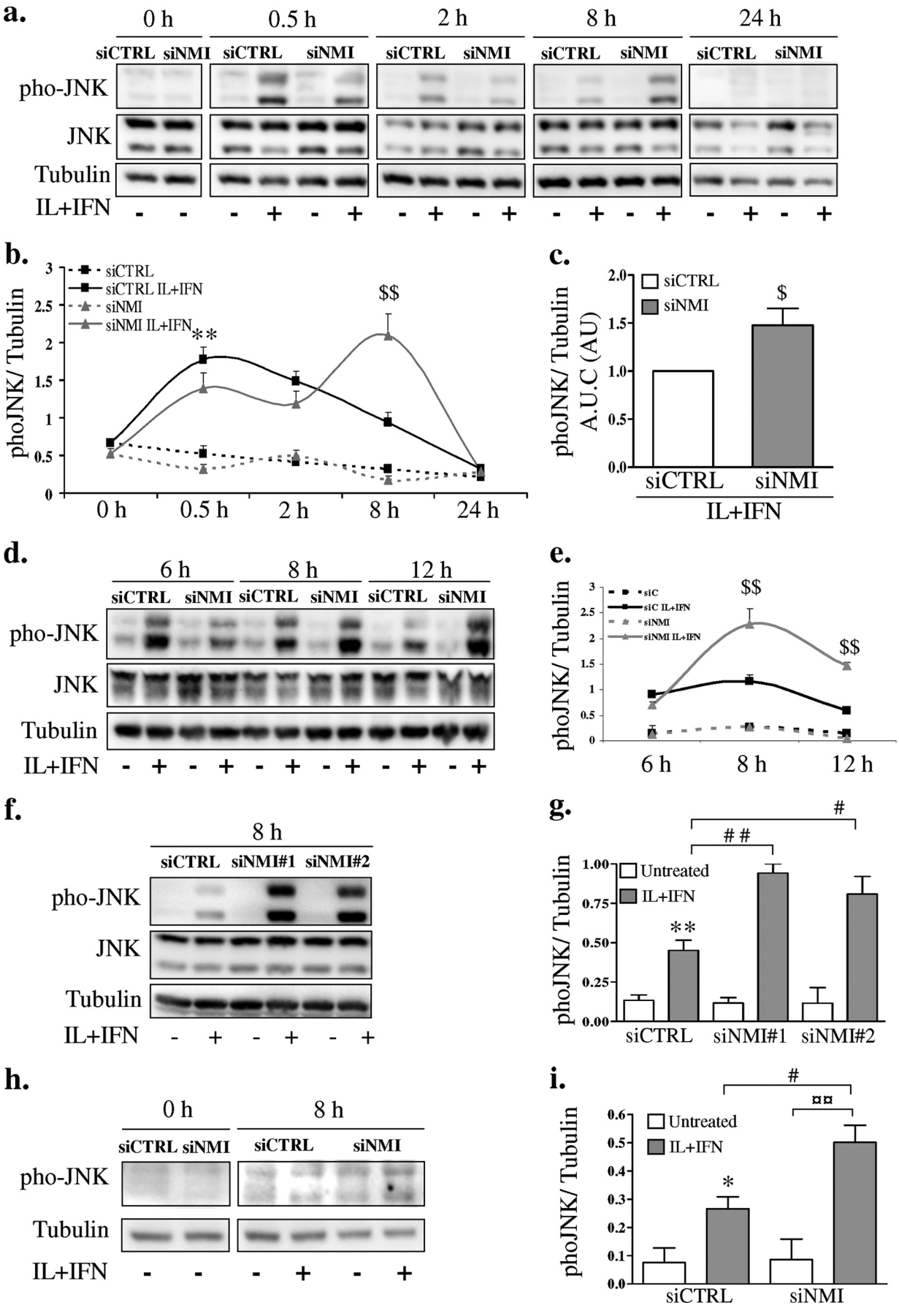
a.
0 h
0.5 h
2 h
8 h
24 h
siCTRL siNMI siCTRL siNMI siCTRL siNMI siCTRL siNMI siCTRL siNMI
pho-JNK
JNK
Tubulin
IL+IFN
b.
siCTRL
siCTRL IL+IFN
siNMI
siNMI IL+IFN
phoJNK/ Tubulin
**
$$
0 h
0.5 h
2 h
8 h
24 h
c.
siCTRL
siNMI
phoJNK/ Tubulin A.U.C (AU)
$
siCTRL
siNMI
IL+IFN
d.
6 h
8 h
12 h
siCTRL siNMI siCTRL siNMI siCTRL siNMI
pho-JNK
JNK
Tubulin
IL+IFN
e.
phoJNK/ Tubulin
$$
$$
6 h
8 h
12 h
f.
8 h
siCTRL siNMI#1 siNMI#2
pho-JNK
JNK
Tubulin
IL+IFN
g.
phoJNK/ Tubulin
Untreated
IL+IFN
#
##
**
siCTRL
siNMI#1
siNMI#2
h.
0 h
8 h
siCTRL siNMI siCTRL siNMI
pho-JNK
Tubulin
IL+IFN
i.
phoJNK/ Tubulin
Untreated
IL+IFN
#
¤¤
*
siCTRL
siNMI

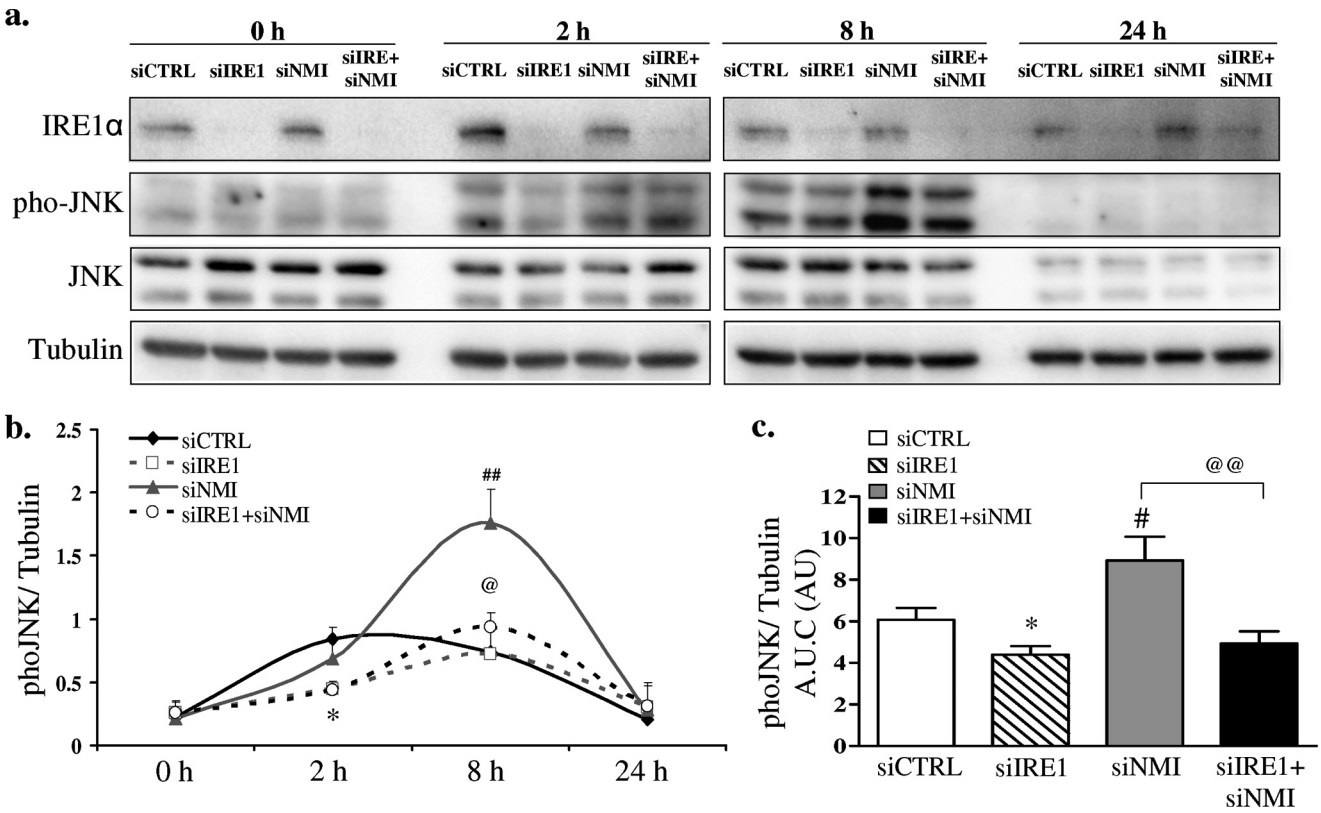

FIGURE 8. **Effect of NMI on JNK phosphorylation is IRE1α-dependent.** INS-1E cells were transfected with siCTRL, siIRE1α, siNMI or co-transfected with siIRE1α + siNMI. After 48 h, cells were incubated with IL-1β + IFN-γ (IL + IFN) and analyzed by Western blot with phospho-specific JNK and total JNK antibodies at the indicated time points. Tubulin expression was used as control for protein loading. One representative Western blot of five independent experiments is shown (*a*). The mean ± S.E. of the optical density measurements of the Western blots following 0, 2, 8, and 24 h IL + IFN exposure is shown (*b*). Quantitative analysis of the area under the curves (*A.U.C.*) of the data shown in *b* for cytokine-treated and siCTRL-transfected cells (siCTRL, *white bar*), IRE1α KD cells (siIRE1, *striped bar*), NMI KD cells (siNMI, *gray bar*), and the double KD cells (siIRE1 + siNMI, *black bar*) is shown in *c*. *, $p < 0.05$ siIRE1 *versus* siCTRL; #, $p < 0.05$, and ##, $p < 0.01$ siNMI *versus* siCTRL; @, $p < 0.05$, and @@, $p < 0.01$ siIRE1 + siNMI *versus* siNMI; one-way ANOVA followed by Student's paired *t* test with Bonferroni correction. Data shown are mean ± S.E. of five independent experiments.

siCTRL and siNMI transfection. *Pdx-1* expression did not change in either INS-1E (Fig. 6*f*) or in dispersed rat islet cells (Fig. 6*l*) following NMI KD.

NMI Modulates IRE1α-dependent JNK activation—IRE1α activation also modifies c-Jun N-terminal kinase (JNK) activity (23), and we next evaluated whether NMI KD interferes with IRE1α-dependent JNK phosphorylation in beta cells. NMI KD increased cytokine-induced JNK phosphorylation in INS-1E cells after 8 and 12 h of exposure (Fig. 7, *a–e*). This was confirmed by quantification of the area under the curves (Fig. 7, *c*). These observations were reproduced using a second siRNA targeting NMI (Fig. 7, *f* and *g*) and were confirmed in FACS-purified rat beta cells (Fig. 7, *h* and *i*). Double KD of NMI and IRE1α reversed the effect of NMI down-regulation on JNK phosphorylation (Fig. 8, *a–c*), confirming the regulatory function of NMI on IRE1α-dependent JNK activation in pancreatic beta cells. Of note, the KD of IRE1α in cytokine-treated cells had a most marked inhibitory effect on JNK activation at 2 h (Fig. 8*b*), indicating a major contribution by IRE1α in the early JNK activation.

NMI-dependent JNK Modulation Regulates Apoptosis in Pancreatic Beta Cells—JNK has an important role for both cytokine- and ER stress-induced beta cell apoptosis (54–58). In line with this, NMI KD increased apoptosis induced by cytokines (Fig. 9*b*) and the ER stressor CPA (Fig. 9*d*) in INS-1E cells and FACS purified rat beta cells (Fig. 9*f*), indicating the involvement of the UPR in the NMI-dependent regulation of apoptosis. Furthermore, NMI KD by two independent siRNAs also augmented apoptosis in human islet cells and the human beta cell line EndoC-βH1, under both basal conditions and follow-

FIGURE 7. **NMI regulates JNK phosphorylation in cytokine-treated INS-1E cells and primary rat beta cells.** INS-1E cells (*a–g*) and FACS-purified rat beta cells (*h* and *i*) were transfected with siCTRL and one (siNMI#1, *a–i*) or two different siRNAs targeting NMI (*f* and *g*, siNMI#1 and siNMI#2). After 48 h, cells were left untreated or treated with IL-1β + IFN-γ (IL + IFN), and proteins were collected at different time points for Western blot analysis with phospho-specific JNK and total JNK antibodies. Tubulin expression was used as control for protein loading. One representative Western blot of five independent experiments in INS-1E cells is shown in *a*, and the mean ± S.E. of the optical density measurements of the Western blots is shown in *b*. Quantitative analysis of the area under the curves (*A.U.C.*) of *b*, expressed as fold induction of the control, confirmed an increase of JNK phosphorylation in IL IFN-treated NMI KD cells (*c*). These findings were confirmed testing the time points 8 and 12 h only (*d* and *e*) and with two different siRNAs targeting NMI (*f* and *g*). One representative Western blot of three independent experiments in INS-1E cells is shown in both *d* and *f*, and the mean ± S.E. of the optical density analysis after IL+IFN exposure is shown in *e* and *g*. One representative Western blot of four independent experiments in FACS-purified rat beta cells is shown in *h*, and the mean ± S.E. of the optical density analysis after 8 h IL + IFN exposure is shown in *i*. *, $p < 0.05$, and **, $p < 0.01$ *versus* untreated; $, $p < 0.05$, and $$, $p < 0.01$ siNMI IL + IFN *versus* siCTRL IL + IFN; #, $p < 0.05$; ##, $p < 0.01$, and ¤¤, $p < 0.01$ as indicated by the *bars*; one-way ANOVA followed by Student's paired *t* test with Bonferroni correction. Data shown are mean ± S.E. of 4–8 independent experiments.

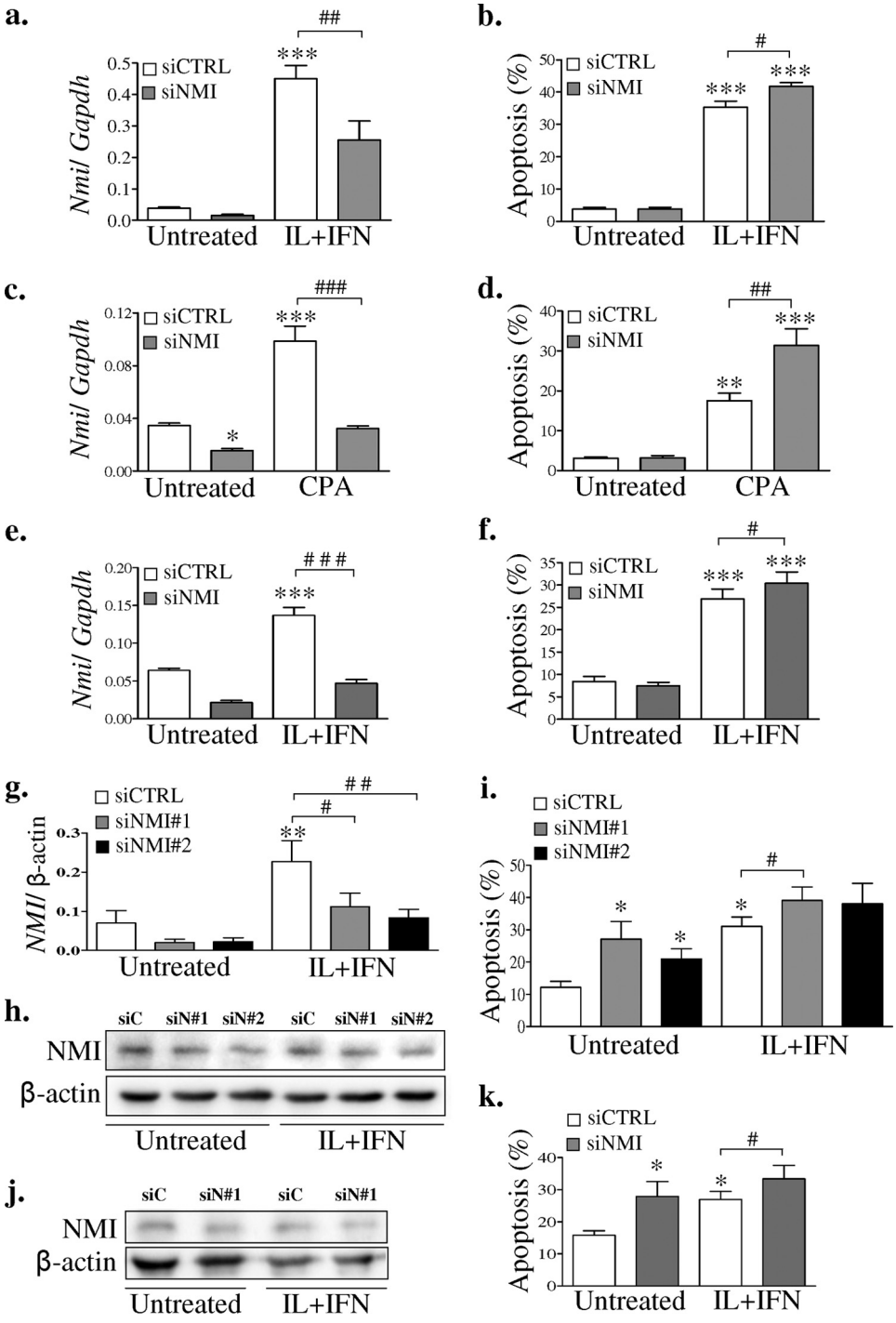

FIGURE 9. **Inhibition of NMI increases ER stress- and cytokine-induced apoptosis in rodent and human beta cells.** INS-1E cells (*a–d*), FACS-purified rat beta cells (*e* and *f*), human islet cells (*g–i*), and the human beta cell line EndoC-βH1 cells (*j* and *k*) were transfected with siCTRL (*white bars*) or one (*a–f, j* and *k*) or two different siNMI (*g–i siNMI#1*, *gray bars* and *siNMI#2*, *black bars*). After 48 h, cells were left untreated or treated with IL-1β + IFN-γ (IL + IFN) or CPA 12.5 μM, as indicated. NMI KD was assessed by RT-PCR (*a, c, e,* and *g*) and Western blot (*h* and *j*) and normalized for the housekeeping gene *Gapdh* (*a, c,* and *e*) or β-actin (*g, h,* and *j*). Apoptosis was evaluated after 24 h of treatment in INS-1E (*b* and *d*) and after 48 h in FACS-purified rat beta cells (*f*), human islet cells (*i*), and the EndoC-βH1 cells (*k*). One representative Western blot of three independent experiments, performed in human islet cells, is shown in *h*. One representative Western blot of four independent experiments, performed in EndoC-βH1 cells, is shown in *j*. *, $p < 0.05$; **, $p < 0.01$, and ***, $p < 0.001$ *versus* siCTRL untreated; #, $p < 0.05$; ##, $p < 0.01$ and ###, $p < 0.001$ as indicated by the *bars*; one-way ANOVA followed by Student's paired *t* test with Bonferroni correction. Results are mean ± S.E. of 4–7 independent experiments. Information on *Nmi/Gapdh* expression (*a*) reproduces information previously shown in Fig. 5, and it is shown again here for clarity.

ing exposure to IL-1β + IFN-γ (Fig. 9, *i* and *k*). The KD of NMI, in the rat models investigated, was ≥50%, as confirmed by RT-PCR (Fig. 9, *a, c,* and *e*) and between 30 and 40% in the human models, as confirmed by RT-PCR (Fig. 9*g*) and Western blot (Fig. 9, *h* and *j*).

We have previously shown that JNK/c-Jun-dependent DP5 expression contributes to apoptosis in cytokine-treated pancreatic beta cells (58). In agreement with these previous results, NMI KD increased c-Jun phosphorylation (Fig. 10, *a* and *b*) and *Dp5* mRNA expression (Fig. 10*c*) in cytokine-treated INS-1E

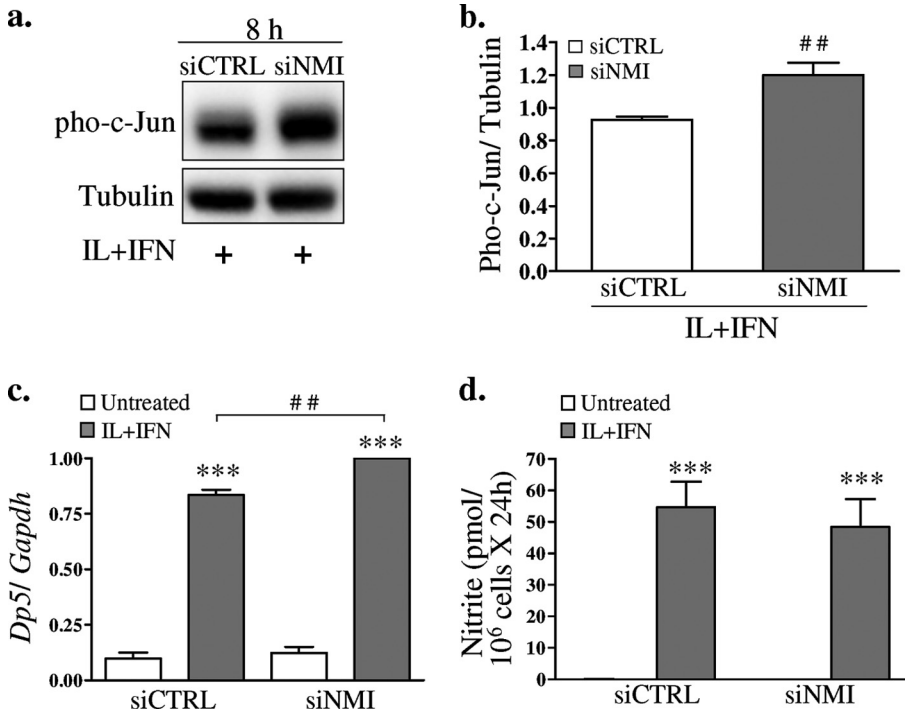

FIGURE 10. **Inhibition of NMI increases c-Jun phosphorylation and DP5 expression, but it does not affect NO production in IL-1β + IFN-γ-treated INS-1E cells.** INS-1E cells were transfected with siCTRL or siNMI. After 48 h, cells were left untreated or treated with IL-1β + IFN-γ (IL + IFN). Proteins were collected after 8 h of IL + IFN incubation for Western blot analysis with a phosphospecific c-Jun antibody (*a*). Total tubulin was used as control for protein loading. One representative Western blot of five independent experiments is shown in *a*, and the mean ± S.E. of the optical density measurements of the Western blots after 8 h IL + IFN exposure is shown in *b*. *Dp5* expression was assessed by RT-PCR, normalized for the housekeeping gene *Gapdh*, after 24 h of IL + IFN incubation (*c*). Supernatants from INS-1E cells were collected after 24 h of IL + IFN treatment and nitrite accumulation in the culture medium evaluated by the Griess method (*d*). ***, $p < 0.001$ *versus* respective untreated, ##, $p < 0.01$ as indicated by the *bars*; paired Student's *t* test. Results are mean ± S.E. of 3–5 independent experiments.

cells. These data suggest that NMI down-regulation in beta cells contributes to apoptosis via the IRE1α-JNK-c-Jun-DP5 pathway.

A possible mechanism for cytokine-induced apoptosis in beta cells is increased nitric oxide production and consequent ER stress (4, 5). NMI KD, however, did not increase nitric oxide production (Fig. 10*d*), making it unlikely that this is a relevant mechanism for beta cell apoptosis following NMI inhibition.

Effect of NMI on JNK Phosphorylation Is Mediated via Modulation of the TRAF2/MKK7 Pathway—IRE1α activates JNK through the binding of the adaptor protein TRAF2 and downstream activation of MKK7 (23). To determine whether TRAF2 is implicated in the observed phospho-JNK increase in NMI-inhibited cells, we used an NMI/TRAF2 double KD approach. NMI/TRAF2 double KD partially reversed the effect of NMI down-regulation on JNK phosphorylation (Fig. 11, *a–c*), suggesting that TRAF2 is partially responsible for the increased JNK phosphorylation observed in NMI-silenced INS-1E cells. MAPK kinase 7 (MKK7) is the main kinase implicated in JNK activation during inflammation (59) and is a target of the apoptosis signal-regulating kinase 1 (ASK1) (60), the kinase downstream of TRAF2 (61). NMI/MKK7 double KD reversed the effect of NMI down-regulation on JNK phosphorylation in cytokine-treated INS-1E cells (Fig. 11, *d–f*). Importantly, it also reduced cytokine-induced beta cell apoptosis in NMI KD cells to the same level observed in siCTR-transfected cells (Fig. 11*g*). These results indicate that NMI KD in pancreatic beta cells increases JNK phosphorylation via the TRAF2/MKK7 pathway.

DISCUSSION

IRE1α is an important regulator of the UPR in pancreatic beta cells, and it may play a key role in the transition from adaptive to pro-apoptotic UPR in T1D (11, 13, 19). The mechanisms regulating IRE1α activation and its signaling for beta cell "adaptation," "stress response," or "apoptosis" remain to be clarified. To address these questions, we presently used a combined "omics" approach based first on an ArrayMAPPIT IRE1α interactome analysis and then comparison of these results against functional genomic analysis of human and rodent beta cells exposed to pro-inflammatory cytokines, as described in Fig. 1. This allowed the identification of NMI as a new cytokine-inducible protein that interacts with IRE1α in pancreatic beta cells. Importantly, increased expression of NMI was also observed in beta cells exposed *in vivo* to the autoimmune assault in NOD mice, a well established model of T1D. Detailed mechanistic studies demonstrated that NMI negatively modulates IRE1α-dependent activation of JNK and apoptosis in rodent and human pancreatic beta cells.

Cytokine exposure induces IRE1α activation in pancreatic beta cells and subsequent *Xbp1* splicing (4), insulin degradation (20, 21, 62), and JNK phosphorylation (54, 58). This early JNK phosphorylation is crucial for the ensuing cytokine-induced apoptosis (54–57, 63). The present observations indicate that

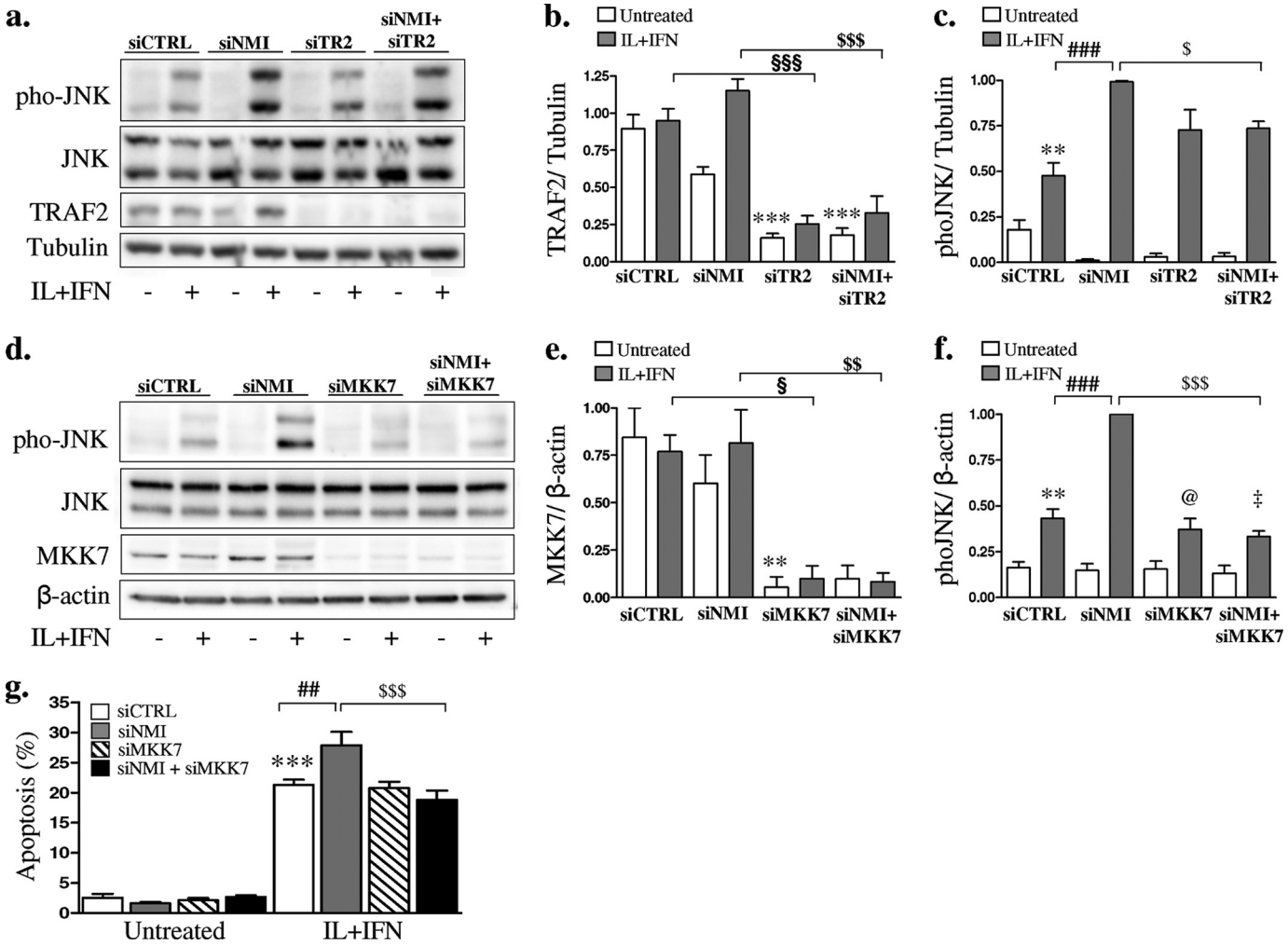

FIGURE 11. **Effect of NMI on JNK phosphorylation and apoptosis is TRAF2/MKK7 pathway-dependent.** INS-1E cells were transfected with siCTRL, siNMI, siTRAF2 (siTR2), or co-transfected with siNMI + siTRAF2 (siNMI + siTR2) (*a–c*). After 48 h, cells were left untreated or incubated with IL-1β + IFN-γ (IL + IFN) for 8 h, and proteins were analyzed by Western blot with phospho-specific JNK, total JNK, and TRAF2 antibodies. Tubulin expression was used as control for protein loading. One representative Western blot of four independent experiments is shown (*a*). The mean ± S.E. of the optical density measurements of the Western blots for TRAF2 (*b*) and phospho-JNK (*c*) are shown. INS-1E cells were transfected with siCTRL, siNMI, siMKK7, or co-transfected with siNMI + siMKK7 (*d–g*). After 48 h, cells were left untreated or incubated with IL-1β + IFN-γ (IL + IFN) for 8 h, and proteins were analyzed by Western blot with phosphospecific JNK, total JNK and MKK7 antibodies. β-Actin expression was used as control for protein loading. One representative Western blot of three independent experiments is shown (*d*). The mean ± S.E. of the optical density measurements of the Western blots for MKK7 (*e*) and phospho-JNK (*f*) are shown. Apoptosis was evaluated after 24 h of incubation with IL-1β + IFN-γ (IL+IFN) treatment (*g*). **, $p < 0.01$ and ***, $p < 0.001$ *versus* siCTRL untreated; @, $p < 0.05$ siMKK7 IL+IFN *versus* siMKK7 untreated; ‡, $p < 0.05$ siNMI + siMKK7 IL+IFN *versus* and siNMI + siMKK7 untreated; ##, $p < 0.01$; ###, $p < 0.001$; $, $p < 0.05$; $$$, $p < 0.001$; §, $p < 0.05$ and §§, $p < 0.01$ as indicated by the *bars*; one-way ANOVA. Data shown are mean ± S.E. of 3–4 independent experiments.

cytokines induce in parallel NMI expression. NMI will bind IRE1α and inhibit the IRE1α/TRAF2/MKK7-dependent activation of JNK, providing a negative feedback for a key pro-apoptotic mechanism in beta cells. Indeed, following NMI KD, IRE1α is not turned off, and the persistent activation of JNK aggravates cytokine-induced apoptosis in pancreatic beta cells via the phospho-c-Jun/DP5 activation pathway.

It has been previously shown that IRE1α-dependent JNK activation is associated with formation of the IRE1α-TRAF2-ASK1 complex and contributes to cell apoptosis caused by pharmacological induction of ER stress (23, 64). We have confirmed these observations in the context of cytokine-induced beta cell apoptosis, and we observed a novel role for NMI in this process. It is conceivable that during cytokine-induced UPR activation, as described for other beta cell stresses (13), cytosolic proteins modulate the induction of IRE1α, fine-tuning the signals provided by accumulation of misfolded proteins in the ER. We have presently identified in NMI a novel fine-tuned modulator of IRE1α, able to regulate both CPA- and cytokine-induced apoptosis in rodent and human pancreatic beta cells. Under the present experimental conditions, the KD of IRE1α inhibits cytokine-induced JNK phosphorylation after only 2 h of cytokine exposure (Fig. 8, *a* and *b*), an early time point that precedes NO production and SERCA-2b inhibition (4). It is thus conceivable that the main role of NMI is to switch off this early cytokine-induced IRE1α-dependent JNK activation, preventing excessive beta cell apoptosis in the context, for instance, of a limited innate immune response. JNK phosphorylation levels decreased in both siCTRL and siNMI after 24 h of cytokine exposure (Fig. 7, *a* and *b*). This maybe due to the cytokine-dependent induction, in parallel with NMI, of other JNK regulators. Our RNA sequencing data of cytokine-treated

human islet cells (30) support this hypothesis, showing a significant up-regulation of several phosphatases such DUSP1 (65) and DUSP16 (66, 67) in IL-1β + IFN-γ-treated islets.

NMI has been shown to potentiate STAT-dependent transcription in other cell types (68). Under our experimental conditions, however, activation of STAT-regulated pathways cannot explain the phenotype induced by NMI KD. Thus, we observed that NMI KD increases cytokine-induced apoptosis in INS-1E and human islet cells, whereas STAT1 KD protects beta cells against cytokine-induced apoptosis (34, 50, 69). Furthermore, STAT1 silencing decreases NO production in cytokine-treated beta cells (50), whereas NMI KD does not change it (Fig. 10*d*).

In conclusion, the discovery of this new role for NMI adds to our understanding of the regulation of key steps of the UPR in stressed beta cells. The present observations indicate that cytokine-induced NMI provides a negative feedback on IRE1α-dependent activation of JNK and apoptosis in beta cells, suggesting a protective role for this protein in the early stages of T1D.

Acknowledgments—We thank A. Musuaya, M. Pangerl, S. Mertens, R. Lemma, C. Dubois, and I. Millard for excellent technical support; Dr. Guy Bottu and Dr. Jean-Valery Turatsinze for the bioinformatic support. We are greatly indebted to Drs. Marc Vidal and David Hill (Center for Cancer Systems Biology), Dana-Farber Cancer Institute (Boston, MA) for making the Center for Cancer Systems Biology ORFeome collection 5.1 available.

REFERENCES

1. Eizirik, D. L., Colli, M. L., and Ortis, F. (2009) The role of inflammation in insulitis and beta cell loss in type 1 diabetes. *Nat. Rev. Endocrinol.* **5,** 219–226
2. Atkinson, M. A., Eisenbarth, G. S., and Michels, A. W. (2014) Type 1 diabetes. *Lancet* **383,** 69–82
3. Santin, I., and Eizirik, D. L. (2013) Candidate genes for type 1 diabetes modulate pancreatic islet inflammation and beta cell apoptosis. *Diabetes Obes. Metab.* **15,** 71–81
4. Cardozo, A. K., Ortis, F., Storling, J., Feng, Y. M., Rasschaert, J., Tonnesen, M., Van Eylen, F., Mandrup-Poulsen, T., Herchuelz, A., and Eizirik, D. L. (2005) Cytokines downregulate the sarcoendoplasmic reticulum pump Ca^{2+} ATPase 2b and deplete endoplasmic reticulum Ca^{2+}, leading to induction of endoplasmic reticulum stress in pancreatic beta cells. *Diabetes* **54,** 452–461
5. Allagnat, F., Fukaya, M., Nogueira, T. C., Delaroche, D., and Welsh, N. (2012) C/EBP homologous protein contributes to cytokine-induced pro-inflammatory responses and apoptosis in beta cells. *Cell Death. Differ.* **19,** 1836–1846
6. Marhfour, I., Lopez, X. M., Lefkaditis, D., Salmon, I., Allagnat, F., Richardson, S. J., Morgan, N. G., and Eizirik, D. L. (2012) Expression of endoplasmic reticulum stress markers in the islets of patients with type 1 diabetes. *Diabetologia* **55,** 2417–2420
7. Tersey, S. A., Nishiki, Y., Templin, A. T., Cabrera, S. M., Stull, N. D., Colvin, S. C., Evans-Molina, C., Rickus, J. L., Maier, B., and Mirmira, R. G. (2012) Islet beta cell endoplasmic reticulum stress precedes the onset of type 1 diabetes in the nonobese diabetic mouse model. *Diabetes* **61,** 818–827
8. Engin, F., Yermalovich, A., Nguyen, T., Hummasti, S., Fu, W., Eizirik, D. L., Mathis, D., and Hotamisligil, G. S. (2013) Restoration of the unfolded protein response in pancreatic beta cells protects mice against type 1 diabetes. *Sci. Transl. Med.* **5,** 10.1126/scitranslmed.3006534
9. Miani, M., Colli, M. L., Ladrière, L., Cnop, M., and Eizirik, D. L. (2012) Mild endoplasmic reticulum stress augments the proinflammatory effect of IL-1β in pancreatic rat beta cells via the IRE1α/XBP1s pathway. *Endocrinology* **153,** 3017–3028
10. Miani, M., Barthson, J., Colli, M. L., Brozzi, F., Cnop, M., and Eizirik, D. L. (2013) Endoplasmic reticulum stress sensitizes pancreatic beta cells to interleukin-1β-induced apoptosis via Bim/A1 imbalance. *Cell Death. Dis.* **4,** e701
11. Eizirik, D. L., Miani, M., and Cardozo, A. K. (2013) Signalling danger: endoplasmic reticulum stress and the unfolded protein response in pancreatic islet inflammation. *Diabetologia* **56,** 234–241
12. Ron, D., and Walter, P. (2007) Signal integration in the endoplasmic reticulum unfolded protein response. *Nat. Rev. Mol. Cell Biol.* **8,** 519–529
13. Eizirik, D. L., and Cnop, M. (2010) ER stress in pancreatic beta cells: the thin red line between adaptation and failure. *Sci. Signal.* **3,** pe7
14. Walter, P., and Ron, D. (2011) The unfolded protein response: from stress pathway to homeostatic regulation. *Science* **334,** 1081–1086
15. Fonseca, S. G., Gromada, J., and Urano, F. (2011) Endoplasmic reticulum stress and pancreatic beta cell death. *Trends Endocrinol. Metab.* **22,** 266–274
16. Gurzov, E. N., and Eizirik, D. L. (2011) Bcl-2 proteins in diabetes: mitochondrial pathways of beta cell death and dysfunction. *Trends Cell Biol.* **21,** 424–431
17. Cnop, M., Welsh, N., Jonas, J. C., Jörns, A., Lenzen, S., and Eizirik, D. L. (2005) echanisms of pancreatic beta cell death in type 1 and type 2 diabetes: many differences, few similarities. *Diabetes* **54,** S97–S107
18. Eizirik, D. L., Cardozo, A. K., and Cnop, M. (2008) The role for endoplasmic reticulum stress in diabetes mellitus. *Endocr. Rev.* **29,** 42–61
19. Woehlbier, U., and Hetz, C. (2011) Modulating stress responses by the UPRosome: a matter of life and death. *Trends Biochem. Sci.* **36,** 329–337
20. Pirot, P., Naamane, N., Libert, F., Magnusson, N. E., Ørntoft, T. F., Cardozo, A. K., and Eizirik, D. L. (2007) Global profiling of genes modified by endoplasmic reticulum stress in pancreatic beta cells reveals the early degradation of insulin mRNAs. *Diabetologia* **50,** 1006–1014
21. Lipson, K. L., Ghosh, R., and Urano, F. (2008) The role of IRE1α in the degradation of insulin mRNA in pancreatic beta cells. *PLoS One* **3,** e1648
22. Hollien, J., and Weissman, J. S. (2006) Decay of endoplasmic reticulum-localized mRNAs during the unfolded protein response. *Science* **313,** 104–107
23. Urano, F., Wang, X., Bertolotti, A., Zhang, Y., Chung, P., Harding, H. P., and Ron, D. (2000) Coupling of stress in the ER to activation of JNK protein kinases by transmembrane protein kinase IRE1. *Science* **287,** 664–666
24. Rodriguez, D. A., Zamorano, S., Lisbona, F., Rojas-Rivera, D., Urra, H., Cubillos-Ruiz, J. R., Armisen, R., Henriquez, D. R., Cheng, E. H., Letek, M., Vaisar, T., Irrazabal, T., Gonzalez-Billault, C., Letai, A., Pimentel-Muiños, F. X., Kroemer, G., and Hetz, C. (2012) BH3-only proteins are part of a regulatory network that control the sustained signalling of the unfolded protein response sensor IRE1α. *EMBO J.* **31,** 2322–2335
25. Qiu, Y., Mao, T., Zhang, Y., Shao, M., You, J., Ding, Q., Chen, Y., Wu, D., Xie, D., Lin, X., Gao, X., Kaufman, R. J., Li, W., and Liu, Y. (2010) A crucial role for RACK1 in the regulation of glucose-stimulated IRE1α activation in pancreatic beta cells. *Sci. Signal.* **3,** ra7
26. Gurzov, E. N., Germano, C. M., Cunha, D. A., Ortis, F., Vanderwinden, J. M., Marchetti, P., Zhang, L., and Eizirik, D. L. (2010) p53 up-regulated modulator of apoptosis (PUMA) activation contributes to pancreatic beta cell apoptosis induced by proinflammatory cytokines and endoplasmic reticulum stress. *J. Biol. Chem.* **285,** 19910–19920
27. Lievens, S., Vanderroost, N., Defever, D., (2012) Van der, H. J., and Tavernier, J. ArrayMAPPIT: a screening platform for human protein interactome analysis. *Methods Mol. Biol.* **812,** 283–294
28. Marchetti, P., Bugliani, M., Lupi, R., Marselli, L., Masini, M., Boggi, U., Filipponi, F., Weir, G. C., Eizirik, D. L., and Cnop, M. (2007) The endoplasmic reticulum in pancreatic beta cells of type 2 diabetes patients. *Diabetologia* **50,** 2486–2494
29. Moore, F., Colli, M. L., Cnop, M., Esteve, M. I., Cardozo, A. K., Cunha, D. A., Bugliani, M., Marchetti, P., and Eizirik, D. L. (2009) PTPN2, a candidate gene for type 1 diabetes, modulates interferon-γ-induced pancreatic beta cell apoptosis. *Diabetes* **58,** 1283–1291
30. Eizirik, D. L., Sammeth, M., Bouckenooghe, T., Bottu, G., Sisino, G., and

others (2012) The human pancreatic islet transcriptome: expression of candidate genes for type 1 diabetes and the impact of pro-inflammatory cytokines. *PLoS Genet.* 10.1371/journal.pgen.1002552
31. Rasschaert, J., Ladrière, L., Urbain, M., Dogusan, Z., Katabua, B., Sato, S., Akira, S., Gysemans, C., Mathieu, C., and Eizirik, D. L. (2005) Toll-like receptor 3 and STAT-1 contribute to double-stranded RNA^+ interferon-γ-induced apoptosis in primary pancreatic beta cells. *J. Biol. Chem.* **280,** 33984–33991
32. Asfari, M., Janjic, D., Meda, P., Li, G., Halban, P. A., and Wollheim, C. B. (1992) Establishment of 2-mercaptoethanol-dependent differentiated insulin-secreting cell lines. *Endocrinology* **130,** 167–178
33. Ravassard, P., Hazhouz, Y., Pechberty, S., Bricout-Neveu, E., Armanet, M., Czernichow, P., and Scharfmann, R. (2011) A genetically engineered human pancreatic beta cell line exhibiting glucose-inducible insulin secretion. *J. Clin. Invest.* **121,** 3589–3597
34. Grieco, F. A., Moore, F., Vigneron, F., Santin, I., Villate, O., Marselli, L., Rondas, D., Korf, H., Overbergh, L., Dotta, F., Marchetti, P., Mathieu, C., and Eizirik, D. L. (2014) IL-17A increases the expression of proinflammatory chemokines in human pancreatic islets. *Diabetologia* **57,** 502–511
35. Eizirik, D. L., and Mandrup-Poulsen, T. (2001) A choice of death–the signal-transduction of immune-mediated beta cell apoptosis. *Diabetologia* **44,** 2115–2133
36. Kutlu, B., Cardozo, A. K., Darville, M. I., Kruhøffer, M., Magnusson, N., Ørntoft, T., and Eizirik, D. L. (2003) Discovery of gene networks regulating cytokine-induced dysfunction and apoptosis in insulin-producing INS-1 cells. *Diabetes* **52,** 2701–2719
37. Ortis, F., Cardozo, A. K., Crispim, D., Störling, J., Mandrup-Poulsen, T., and Eizirik, D. L. (2006) Cytokine-induced proapoptotic gene expression in insulin-producing cells is related to rapid, sustained, and nonoscillatory nuclear factor-κB activation. *Mol. Endocrinol.* **20,** 1867–1879
38. Eizirik, D. L., Pipeleers, D. G., Ling, Z., Welsh, N., Hellerström, C., and Andersson, A. (1994) Major species differences between humans and rodents in the susceptibility to pancreatic beta cell injury. *Proc. Natl. Acad. Sci. U.S.A.* **91,** 9253–9256
39. Eizirik, D. L., Sandler, S., Welsh, N., Cetkovic-Cvrlje, M., Nieman, A., Geller, D. A., Pipeleers, D. G., Bendtzen, K., and Hellerström, C. (1994) Cytokines suppress human islet function irrespective of their effects on nitric oxide generation. *J. Clin. Invest.* **93,** 1968–1974
40. Schulz, K., Kerber, S., and Kelm, M. (1999) Reevaluation of the Griess method for determining NO/NO2-in aqueous and protein-containing samples. *Nitric Oxide* **3,** 225–234
41. Eyckerman, S., Verhee, A., der Heyden, J. V., Lemmens, I., Ostade, X. V., Vandekerckhove, J., and Tavernier, J. (2001) Design and application of a cytokine-receptor-based interaction trap. *Nat. Cell Biol.* **3,** 1114–1119
42. Lievens, S., Vanderroost, N., Van der Heyden, J., Gesellchen, V., Vidal, M., and Tavernier, J. (2009) Array MAPPIT: high-throughput interactome analysis in mammalian cells. *J. Proteome Res.* **8,** 877–886
43. Moore, F., Cunha, D. A., Mulder, H., and Eizirik, D. L. (2012) Use of RNA interference to investigate cytokine signal transduction in pancreatic beta cells. *Methods Mol. Biol.* **820,** 179–194
44. Moore, F., Santin, I., Nogueira, T. C., Gurzov, E. N., Marselli, L., Marchetti, P., and Eizirik, D. L. (2012) The transcription factor C/EBPδ has anti-apoptotic and anti-inflammatory roles in pancreatic beta cells. *PLoS One* 10.1371/journal.pone.0031062
45. Cunha, D. A., Hekerman, P., Ladrière, L., Bazarra-Castro, A., Ortis, F., Wakeham, M. C., Moore, F., Rasschaert, J., Cardozo, A. K., Bellomo, E., Overbergh, L., Mathieu, C., Lupi, R., Hai, T., Herchuelz, A., Marchetti, P., Rutter, G. A., Eizirik, D. L., and Cnop, M. (2008) Initiation and execution of lipotoxic ER stress in pancreatic beta cells. *J. Cell Sci.* **121,** 2308–2318
46. Hoorens, A., Van de Casteele, M., Klöppel, G., and Pipeleers, D. (1996) Glucose promotes survival of rat pancreatic beta cells by activating synthesis of proteins which suppress a constitutive apoptotic program. *J. Clin. Invest.* **98,** 1568–1574
47. Chen, M. C., Proost, P., Gysemans, C., Mathieu, C., and Eizirik, D. L. (2001) Monocyte chemoattractant protein-1 is expressed in pancreatic islets from prediabetic NOD mice and in interleukin-1β-exposed human and rat islet cells. *Diabetologia* **44,** 325–332
48. Overbergh, L., Valckx, D., Waer, M., and Mathieu, C. (1999) Quantification of murine cytokine mRNAs using real time quantitative reverse transcriptase PCR. *Cytokine* **11,** 305–312
49. Cardozo, A. K., Kruhøffer, M., Leeman, R., Orntoft, T., and Eizirik, D. L. (2001) Identification of novel cytokine-induced genes in pancreatic beta cells by high-density oligonucleotide arrays. *Diabetes* **50,** 909–920
50. Moore, F., Naamane, N., Colli, M. L., Bouckenooghe, T., Ortis, F., Gurzov, E. N., Igoillo-Esteve, M., Mathieu, C., Bontempi, G., Thykjaer, T., Ørntoft, T. F., and Eizirik, D. L. (2011) STAT1 is a master regulator of pancreatic beta cell apoptosis and islet inflammation. *J. Biol. Chem.* **286,** 929–941
51. Ortis, F., Naamane, N., Flamez, D., Ladrière, L., Moore, F., Cunha, D. A., Colli, M. L., Thykjaer, T., Thorsen, K., Orntoft, T. F., and Eizirik, D. L. (2010) Cytokines interleukin-1β and tumor necrosis factor-α regulate different transcriptional and alternative splicing networks in primary beta cells. *Diabetes* **59,** 358–374
52. Tirasophon, W., Lee, K., Callaghan, B., Welihinda, A., and Kaufman, R. J. (2000) The endoribonuclease activity of mammalian IRE1 autoregulates its mRNA and is required for the unfolded protein response. *Genes Dev.* **14,** 2725–2736
53. Bendelac, A., Carnaud, C., Boitard, C., and Bach, J. F. (1987) Syngeneic transfer of autoimmune diabetes from diabetic NOD mice to healthy neonates. Requirement for both $L3T4^+$ and $Lyt\text{-}2^+$ T cells. *J. Exp. Med.* **166,** 823–832
54. Ammendrup, A., Maillard, A., Nielsen, K., Aabenhus Andersen, N., Serup, P., Dragsbaek Madsen, O., Mandrup-Poulsen, T., and Bonny, C. (2000) The c-Jun amino-terminal kinase pathway is preferentially activated by interleukin-1 and controls apoptosis in differentiating pancreatic beta cells. *Diabetes* **49,** 1468–1476
55. Bonny, C., Oberson, A., Steinmann, M., Schorderet, D. F., Nicod, P., and Waeber, G. (2000) IB1 reduces cytokine-induced apoptosis of insulin-secreting cells. *J. Biol. Chem.* **275,** 16466–16472
56. Bonny, C., Oberson, A., Negri, S., Sauser, C., and Schorderet, D. F. (2001) Cell-permeable peptide inhibitors of JNK: novel blockers of beta cell death. *Diabetes* **50,** 77–82
57. Marroqui, L., Santin, I., Dos Santos, R. S., Marselli, L., Marchetti, P., and Eizirik, D. L. (2014) BACH2, a candidate risk gene for type 1 diabetes, regulates apoptosis in pancreatic beta cells via JNK1 modulation and crosstalk with the candidate gene PTPN2. *Diabetes* **63,** 2516–2527
58. Gurzov, E. N., Ortis, F., Cunha, D. A., Gosset, G., Li, M., Cardozo, A. K., and Eizirik, D. L. (2009) Signaling by IL-1β+IFN-γ and ER stress converge on DP5/Hrk activation: a novel mechanism for pancreatic beta cell apoptosis. *Cell Death Differ.* **16,** 1539–1550
59. Lee, S. I., Boyle, D. L., Berdeja, A., and Firestein, G. S. (2012) Regulation of inflammatory arthritis by the upstream kinase mitogen activated protein kinase kinase 7 in the c-Jun N-terminal kinase pathway. *Arthritis Res. Ther.* **14,** R38
60. Matsuzawa, A., Nishitoh, H., Tobiume, K., Takeda, K., and Ichijo, H. (2002) Physiological roles of ASK1-mediated signal transduction in oxidative stress- and endoplasmic reticulum stress-induced apoptosis: advanced findings from ASK1 knockout mice. *Antioxid. Redox Signal.* **4,** 415–425
61. Nishitoh, H., Saitoh, M., Mochida, Y., Takeda, K., Nakano, H., Rothe, M., Miyazono, K., and Ichijo, H. (1998) ASK1 is essential for JNK/SAPK activation by TRAF2. *Mol. Cell* **2,** 389–395
62. Han, D., Lerner, A. G., Vande Walle, L., Upton, J. P., Xu, W., Hagen, A., Backes, B. J., Oakes, S. A., and Papa, F. R. (2009) IRE1α kinase activation modes control alternate endoribonuclease outputs to determine divergent cell fates. *Cell* **138,** 562–575
63. Santin, I., Moore, F., Colli, M. L., Gurzov, E. N., Marselli, L., Marchetti, P., and Eizirik, D. L. (2011) PTPN2, a candidate gene for type 1 diabetes, modulates pancreatic beta cell apoptosis via regulation of the BH3-only protein Bim. *Diabetes* **60,** 3279–3288
64. Nishitoh, H., Matsuzawa, A., Tobiume, K., Saegusa, K., Takeda, K., Inoue, K., Hori, S., Kakizuka, A., and Ichijo, H. (2002) ASK1 is essential for endoplasmic reticulum stress-induced neuronal cell death triggered by expanded polyglutamine repeats. *Genes Dev.* **16,** 1345–1355

65. Koga, S., Kojima, S., Kishimoto, T., Kuwabara, S., and Yamaguchi, A. (2012) Overexpression of MAP kinase phosphatase-1 (MKP-1) suppresses neuronal death through regulating JNK signaling in hypoxia/re-oxygenation. *Brain Res.* **1436,** 137–146
66. Kim, K. H., An, D. R., Song, J., Yoon, J. Y., Kim, H. S., Yoon, H. J., Im, H. N., Kim, J., Kim, do, J., Lee, S. J., Kim, K. H., Lee, H. M., Kim, H. J., Jo, E. K., Lee, J. Y., and Suh, S. W. (2012) *Mycobacterium tuberculosis* Eis protein initiates suppression of host immune responses by acetylation of DUSP16/MKP-7. *Proc. Natl. Acad. Sci. U.S.A.* **109,** 7729–7734
67. Lee, S., Syed, N., Taylor, J., Smith, P., Griffin, B., Baens, M., Bai, M., Bourantas, K., Stebbing, J., Naresh, K., Nelson, M., Tuthill, M., Bower, M., Hatzimichael, E., and Crook, T. (2010) DUSP16 is an epigenetically regulated determinant of JNK signalling in Burkitt's lymphoma. *Br. J. Cancer* **103,** 265–274
68. Zhu, M., John, S., Berg, M., and Leonard, W. J. (1999) Functional association of Nmi with Stat5 and Stat1 in IL-2- and IFNγ-mediated signaling. *Cell* **96,** 121–130
69. Gysemans, C. A., Ladrière, L., Callewaert, H., Rasschaert, J., Flamez, D., Levy, D. E., Matthys, P., Eizirik, D. L., and Mathieu, C. (2005) Disruption of the γ-interferon signaling pathway at the level of signal transducer and activator of transcription-1 prevents immune destruction of beta cells. *Diabetes* **54,** 2396–2403